KeAi

CHINESE ROOTS
GLOBAL IMPACT

Contents lists available at ScienceDirect

Petroleum Science

journal homepage: www.keaipublishing.com/en/journals/petroleum-science



Original Paper

Differences in hydrocarbon accumulation and controlling factors of slope belt in graben basin: A case study of Pinghu Slope Belt in the Xihu sag of the east China Sea Shelf basin (ECSSB)



Bo Yan ^a, Hong-Qi Yuan ^{b, *}, Ning Li ^c, Wei Zou ^c, Peng Sun ^c, Meng Li ^b, Yue-Yun Zhao ^b, Qian Zhao ^b

- ^a College of Earth Sciences, Jilin University, Changchun, 130061, Jilin, China
- ^b School of Geosciences, Northeast Petroleum University, Daqing, 163318, Heilongjiang, China
- ^c Research Institute of CNOOC Shanghai Branch, Shanghai, 200030, China

ARTICLE INFO

Article history: Received 10 June 2023 Received in revised form 5 December 2023 Accepted 8 June 2024 Available online 11 June 2024

Edited by Jie Hao and Teng Zhu

Keywords:
East China Sea Shelf Basin (ECSSB)
Pinghu slope belt
Variation in hydrocarbon accumulation
Controlling factors of hydrocarbon
accumulation
Hydrocarbon accumulation pattern

ABSTRACT

The Pinghu slope belt in the Xihu sag of the East China Sea Shelf Basin (ECSSB) is a crucial hydrocarbon production area in eastern China. However, due to the complex geological conditions, publications have lacked comprehensive research on the spatial-temporal coupling relationships of primary factors that impact hydrocarbon accumulation in the Pinghu slope belt. Furthermore, the hydrocarbon distribution patterns and the controlling factors across different study areas within the same slope belt are not yet fully understood. This study extensively utilized three-dimensional seismic data, well logging data, geochemical analysis, fluorescence analysis, and oil testing and production data to address these issues. Following a "stratification and differentiation" approach, the study identified seven distinct hydrocarbon migration and accumulation units (HMAU) in the Pinghu slope area based on the structural morphology characteristics, hydrocarbon source-reservoir-cap rock patterns, hydrocarbon migration pathways, and hydrocarbon supply range. Detailed analysis was conducted to examine the hydrocarbon distribution patterns and controlling factors within each migration and accumulation unit across different structural units, including high, medium, and low structural components. All data sources support a "southernnorthern sub-area division, eastern-western sub-belt division, and variations in hydrocarbon accumulation" pattern in the Pinghu slope belt. The degree of hydrocarbon accumulation is controlled by the factors of structural morphology, hydrocarbon generation potential of source rocks, the spatial position of source slopes, fault sealing capacity, and sand body distribution. Furthermore, different coupling patterns of faults and sand bodies play a pivotal role in governing hydrocarbon enrichment systems across various migration and accumulation units. These observations indicate that three hydrocarbon accumulation patterns have been established within the slope belt, including near-source to far-source gentle slope with multiple hydrocarbon kitchens in the XP1-XP4 zones, near-source to middle-source gentle slope with dual-hydrocarbon kitchens in the XP5 zone, and near-source steep slope with a single hydrocarbon kitchen in the XP6-XP7 zones. These findings contribute to enhancing the theoretical system of hydrocarbon accumulation in the slope belt.

© 2024 The Authors. Publishing services by Elsevier B.V. on behalf of KeAi Communications Co. Ltd. This is an open access article under the CC BY-NC-ND license (http://creativecommons.org/licenses/by-nc-nd/

4.0/).

1. Introduction

Oil and gas production in the graben basins holds a dominant position among the proven hydrocarbon reserves. Compared to

* Corresponding author.

E-mail address: yuanhongqi@nepu.edu.cn (H.-Q. Yuan).

marine graben basins prevalent in other countries for oil and gas exploration and development, terrestrial graben basins are the most significant basin types for oil and gas in eastern China and play a significant role in hydrocarbon exploration (Hou et al., 2019; Wang et al., 2020; Yan et al., 2022; Zhang et al., 2023). The widely distributed graben basins in eastern China are predominantly formed under extensional tectonic settings, exhibiting distinct structural characteristics. These basins are primarily categorized as

half-graben with one fault and graben with two faults, with halfgraben being the most prevalent type (Bailey et al., 2006; Pánek and Klimeš, 2016). Generally, slope belts are graben basins, and half-graben serves as a crucial secondary structure unit, possessing favorable conditions for hydrocarbon accumulation. These favorable conditions include proximity to hydrocarbon generation centers in deep sag, favorable reservoir properties, widely distributed hydrocarbon traps, and diverse types of cap rocks and migration systems. Slope belts function as long-term hydrocarbon migration pathways and favorable sites for hydrocarbon accumulation, and their favorable conditions determine their extensive exploration prospects (Li et al., 2022; Liu et al., 2018; Wang et al., 2017; Zhou et al., 2019). Previous research has primarily focused on the genetic mechanisms, morphology, structure, distribution characteristics, and other comprehensive factors associated with slope belts in various types of terrestrial graben basins and classified the slope belts (refer to Table 1). Subsequently, investigations have delved into the characteristics and controlling factors of hydrocarbon accumulation.

Regarding studies of hydrocarbon accumulation in slope belts, it is generally accepted that favorable hydrocarbon shows occur at upper slope structures distanced from the deep sag zones (Liu et al., 2020). These upper positions also align with the preferential direction of hydrocarbon migration (Liang et al., 2020; Meng et al., 2020; Zhao et al., 2016). Simultaneously, the lower slopes near

the deep sag zones often develop the gravity current dominated sand bodies. Due to their proximity to deep sag for hydrocarbon accumulation, these lower positions are considered favorable areas for hydrocarbon accumulation (Zhou et al., 2019). Reservoirs are superposed with or interbedded within source rocks in vertical directions, and hydrocarbons are either close to or distributed within the source rocks. Horizontally, hydrocarbons accumulate inside or around source rocks, forming hydrocarbon expulsion centers, as observed in North American regions such as the Piceance Basin (Cumella et al., 2017; Tong et al., 2017), Devonian Appalachian Basin (Engelder et al., 2009; Chabalala et al., 2020), Illinois Basin (Greb et al., 2020), and Michigan Basin (Adeyilola et al., 2022). However, long-time exploration experience has revealed that hydrocarbon accumulation locations in slope belts often do not align with the tradition understanding of upper positions within structures or the nearest sandstone layers to the source rocks, for instance, the LS36-1 structural belt in the Lishui Sag of the East China Sea Basin and the LF35-1 structural belt in the Pearl River Mouth Basin. Early theories on hydrocarbon accumulation primarily focused on studying the conditions for hydrocarbon accumulation, including the "Source Control Theory" (Hu, 1982), "Zone Control Theory" (Hu et al., 1986), "Facies Control Theory" (Zou et al., 2005), "Hydrocarbon Accumulation in Sag Theory" (Yang et al., 2023), and "Sag-wide Oil-Bearing Theory" (Zhao et al., 2004). Later, research focused on specific controlling

Table 1Classification of the slope belts in terrestrial graben basins.

Classification		Gentle Slope Belt Types	Reference
Morphology Features	Gentle slope belt	Inherited erosion type, Inherited overlap type, Structural slope, Concave-oblique type	Liu and Fang (1988)
	Planar and Cross-section	Complex type (two categories, ten types), Simple type	Li et al. (2001)
Structural	Stratigraphic Development	Dual-type, Wide gentle type, Narrow steep type	Li et al. (2004
Features	Structure	Wide gentle type, Narrow steep type, Dual type	Qin et al. (2003)
		Terraced-slope type, Inherited type, Sag-slope type	Wang et al. (2006)
	Development Degree of Fault	Complex type (two types), Simple type	Fu et al. (2006)
	Development Degree of Basement Fault	Fault terrace style, Slope fold style, Half-graben style, Graben style	Zhang (2005)
	Fault Combination	Half-graben style, Slope fold style, Fault terrace style	Wang and Xian (2006)
Genesis Mechanism	Structural Evolution and Sedimentary	Sedimentary type, Structural-sedimentary type, Structural type	Fei (1999)
	Characteristics	Sedimentary type, Structural type, Structural-sedimentary type	Zhai and He (2005)
	Geological Structure	Graben type, Monocline type	Yuan and Jiao (2002)
	Structural Factors	Slope type, Single-terrace type, Multi-terrace type	Yu et al. (2007)
	Structural Evolution	Sedimentary forming type, Erosion landform type, Structural type	Fan et al. (2008)
		Synsedimentary type, Structural type, Superimposed type	Jin et al. (2009)
Comprehensive Factors	Structural Evolution and Geomorphic Features	Single fault-sedimentary slope fold type, Single fault-slope type, Double faults-sedimentary slope break type	Peng (2005)
	Genesis and Fault Slope Pattern	Structural fold, Sedimentary fold, Erosion fold	Yuan (2007)
	Genesis, Width, Dip Angle	Tilting structural type, Sedimentary-Structural composite type, Inversion type	Dong et al. (2019)
	Genesis-Structure	Multi-terrace flexural slope, Terraced fault slope, Monocline slope and rotated tilting slope	Dong et al. (2014)
		Flexural slope fold type, Gentle terraced-slope type, Wide gentle fault terrace type, Narrow steep fault stepped terrace type, Tilting flexural type	Zhao et al. (2016)
	Structural Evolution and Fault Slope	Synsedimentary gentle oblique fault slope type, Synsedimentary stable fault terrace type	Xue et al. (2016)
	Source Rock, Sedimentation, Hydrocarbon Accumulation Variation	High slope, Medium slope, Low slope	Zhao et al. (2017)
	Structure Activity、Basement Fault Pattern	Simple type, Transitional type, Complex type	Zhao et al. (2019)
	Basement Subsidence and Fault Activity	Subsidence type, Structural type, Inversion type	Liu et al. (2022)

factors, emphasizing the integration of multiple factors or conducting studies on key factors. Thus, the findings of these studies facilitated the development of theories and understandings such as "Unconventional Hydrocarbon Accumulation Theories" (Jia, 2017; Martini et al., 1998; Song et al., 2017), "Hydrocarbon Accumulation In Anticlinal Trapping Theories" (Li et al., 2021), "Fault-Controlled Hydrocarbon Accumulation Theories" (Luo, 2010), "Hydrocarbon Accumulation In Carbonate Reservoir Theories" (Zhou et al., 2022). Attention has gradually shifted towards the exploration and development of non-structural reservoirs, particularly those related to strata, lithology, and structure-lithology. Exploration targets have become increasingly concealed, making the research of characteristics and controlling factors of hydrocarbon accumulation in slope belts particularly urgent (Alves et al., 2020; Chen et al., 2018; Fu et al., 2023; Kordi, 2019; Lao et al., 2019; Liu et al., 2022; Zeng et al., 2022).

The Pinghu slope belt is one of the sag types with relatively abundant offshore hydrocarbon resources and excellent exploration potential in China. Currently, due to limited data and understanding of exploration, petroleum geology research in the Pinghu slope belt is relatively incomplete compared to other China Seas. The theoretical systems and methods for the exploration of hydrocarbons in this region are still being gradually developed. Previous studies have rarely focused on the comprehensive multiple factor analysis of slope belts. In recent years, research on the hydrocarbon distribution patterns and main controlling factors of hydrocarbon accumulation in the Pinghu slope belt of the Xihu Sag in the ECSSB has relied chiefly on static analyses based on a single factor, such as the development characteristics of source rocks (Ma et al., 2020; Quan et al., 2022), the oil generation model of the liptinite-rich coals (Li et al., 2022), tectonic evolution (Abbas et al., 2018), the influence of fault-controlled traps (Sun et al., 2022), fault activity analysis (Zhang et al., 2023), provenance division and spatiotemporal evolution (Zhao et al., 2021), sequence stratigraphy evolution (Li et al., 2014), sedimentary system evolution and characteristics of sand body distribution (Chen et al., 2022; Hu et al., 2020; Jiang et al., 2022), physical properties of reservoirs (Wang et al., 2020; Zeng et al., 2021), characteristics of cap rocks and evaluation of fault sealing capacity (Guan et al., 2022), and direction and preservation conditions governing hydrocarbon migration and accumulation (Liu et al., 2019; Liu and Zhang, 2021). Based on the analysis of existing data and previous research in the target area, this study identifies the following unresolved issues: 1. In-depth investigation is needed regarding the spatial-temporal configuration relationship of the essential factors for hydrocarbon accumulation in the Pinghu slope belt. 2. The hydrocarbon distribution patterns and main controlling factors of hydrocarbon accumulation in different research areas within the same slope belt have not been clarified, lacking comparative studies on the characteristics of hydrocarbon accumulation. These two issues severely limit hydrocarbon exploration in this region. For the first time in the region, this study divides the HAMU units based on structural morphology characteristics, hydrocarbon source-reservoir-cap rock patterns, hydrocarbon migration pathways, and hydrocarbon supply range. It thoroughly discusses the distribution patterns and main controlling factors of hydrocarbons in different structural units within the migration and accumulation units (upper, medium, and lower), establishing hydrocarbon accumulation patterns. Furthermore, coupling the effects of structural morphology, hydrocarbon generation potential of source rocks, the spatial position of source slopes, fault sealing capacity, and sand body distribution, this study investigates the controlling factors of hydrocarbon accumulation between different hydrocarbon migration and accumulation in the target area. We comprehensively evaluated and analyzed the controlling factors of hydrocarbon accumulation in

the slope belt. Finally, this study established a "stratification and differentiation" approach to classify hydrocarbon accumulation systems for complex reservoirs in the slope belt using the multifactor coupling, aiming to improve the understanding of hydrocarbon accumulation in the ECSSB. The findings of this research provide strong evidence for the breakthrough of hydrocarbon exploration potential in this region and offer theoretical guidance for offshore hydrocarbon exploration in China Seas.

2. Geological setting

The East China Sea Shelf Basin (ECSSB) is a Mesozoic-Cenozoic post-arc continental margin graben-depression basin developed on the Pre-Sinian basement, belonging to the southeastern margin of the Eurasian Plate (Suo et al., 2019; Zhang et al., 2018; Zhou et al., 2019; Zhu et al., 2019) (as shown in Fig. 1a). The Xihu Sag is located in the northeastern part of the ECSSB, with a length of approximately 460 km and a width in the range of 75-130 km. It covers an area of up to $5 \times 10^4 \text{ km}^2$ and is a long and narrow Cenozoic sedimentary sag oriented in the NNE direction. Since the Late Mesozoic, due to the direct impact of the Pacific Plate and the Philippine Plate and the indirect influence of the collision between the Indian-Eurasian Plates, the regional stress field in the ECSSB has undergone multiple changes (Morley, 2012; Niu et al., 2015; Shang et al., 2017), resulting in the "eastern-western sub-belt division and southern-northern sub-area division" characteristics of the Xihu Sag (Yang et al., 2020) (Fig. 1b). As one of the main study areas in the ECSSB, the sedimentary characteristics of the Xihu Sag are similar to those of the entire basin and exhibit a structural evolution pattern of faulting followed by sag (Suo et al., 2015; Zhang et al., 2016). The Xihu Sag can be divided from west to east into multiple secondary structure units, including the western slope belt, western sub-sag, central inversion structural belt, eastern subsag, and eastern fault terrace belt (Liu et al., 2019; Xu et al., 2020) (as shown in Fig. 1c).

The Pinghu slope belt is located in the central part of the western slope zone of the Xihu Sag, with an area of approximately 6,000 km². It can be further divided from west to east into the upper, medium, and lower slope belts (Fig. 1d) (Jiang, 2019). The study area is mainly characterized by five major structural transition zones, which have an overall NNW-SSE trend and intersect the regional extensional system at a low angle. However, the strike-slip features are not significant, and no large-scale strike-slip faults are formed in the shallow section, indicating a small volume of strike-slip faults existing in the region, primarily acting as segmentation faults (Hu et al., 2018). Due to the impact of the strike-slip, the Pinghu slope belt exhibits a divisional deformation feature (Fig. 1e).

The primary sedimentary period of the Pinghu Slope Belt is the Paleogene, characterized by clastic sedimentation. The sedimentary strata (Fig. 2) can be divided from bottom to top into the Paleocene (E_1) , Baoshi Formation (E_2bs) of the lower to middle Eocene, Pinghu Formation (E_2p) of the middle to upper Eocene, Huagang Formation (E_3h) of the Oligocene, Longjing Formation (N_1^1l) , Yuquan Formation (N_1^2y) , and Liulang Formation (N_1^3l) of the Miocene, Santan Formation (N2s) of the Pliocene, and Donghai Group (Qd) of the Quaternary (Wang et al., 2018; Xu et al., 2020). This study focuses on the Pinghu Formation in the main study area, which can be further divided from bottom to top into two beds of the lower Pinghu Formation (P9–P10), two beds of the middle-lower sub-member of the Pinghu Formation (P7-P8), two beds of the middle-upper submember of the Pinghu Formation (P5-P6), and four beds of the upper Pinghu Formation (P1-P4). The upper part of the Pinghu Formation forms tidal deltas. In contrast, the lower part shows distinct tidal flat sediment characteristics, with well-developed sand bodies such as tidal channels and sand flats. Overall, the

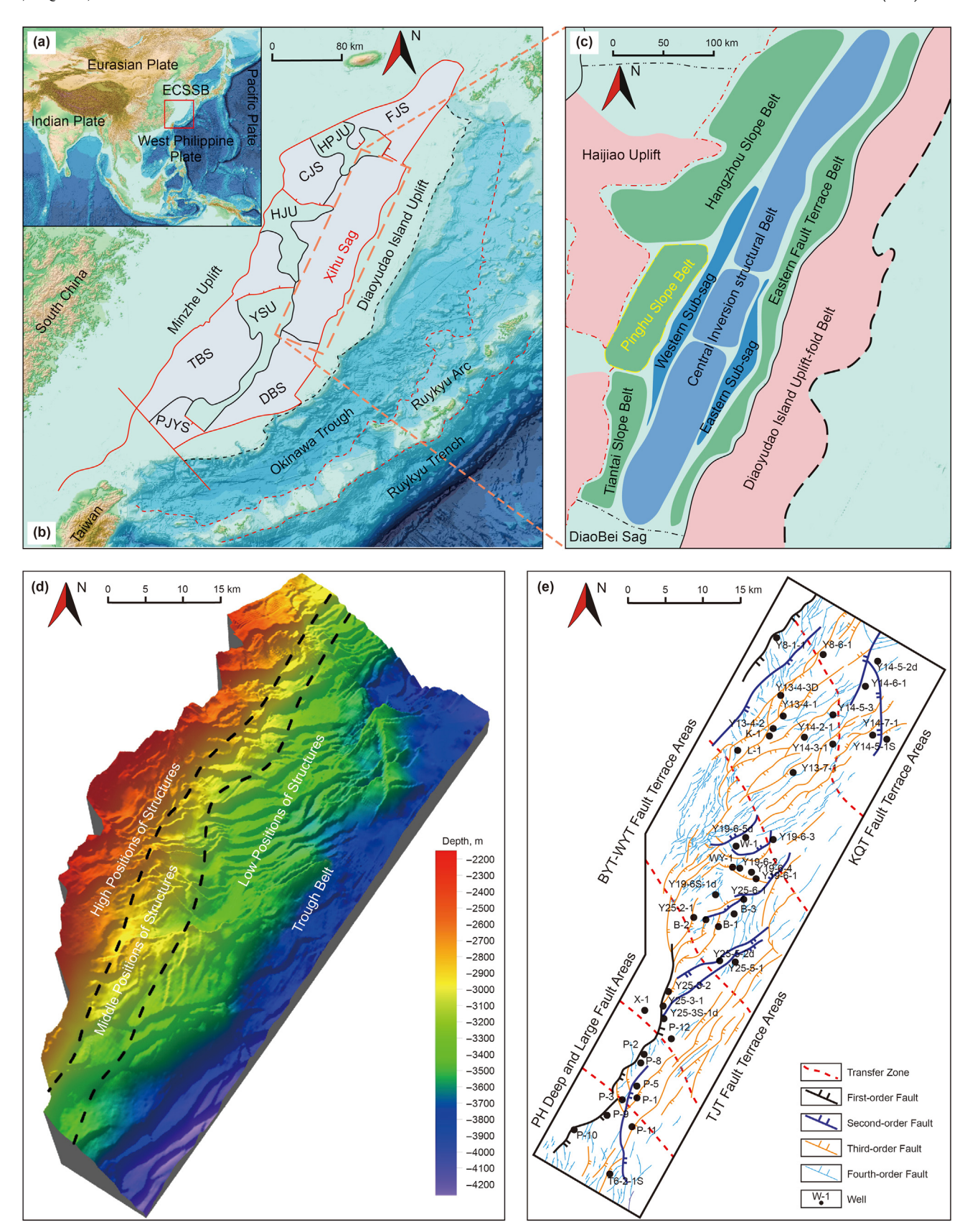


Fig. 1. (a) Regional tectonic location of the ECSSB. (b) Structural unit sketch map of the ECSSB delineates the location of the Xihu Sag within the ECSSB. (c) A schematic map details the location and structural divisions of the Xihu Sag, showing the location of the Pinghu slope belt in the Xihu Sag. (d) Structural geomorphology of the Pinghu Formation in the Pinghu slope belt, Fault system of $T3^2$ seismic interface (the boundary between the lower interval of E_2P_2 and upper interval of E_2P_1) outlines the fault distribution of the Pinghu slope belt in the Xihu Sag. Abbreviation: East China Sea Shelf Basin (ECSSB), Fujiang Sag (FJS), Changjiang Sag (CJS), Taibei Sag (TBS), Diaobei Sag (DBS), Pengjiayu Sag (PJYS), Hupijiao Uplift (HJJU), Yushan Uplift (YSU).

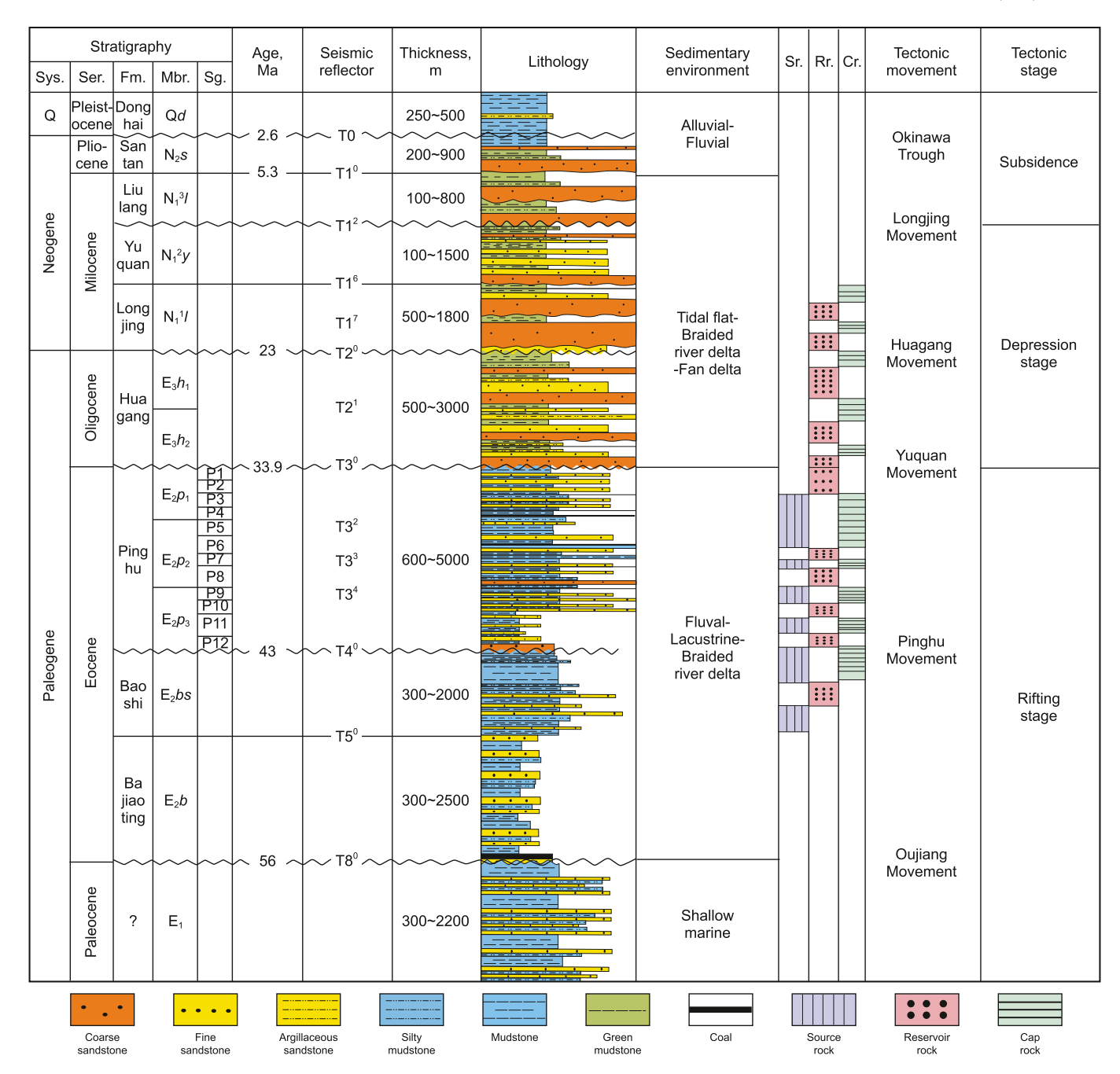


Fig. 2. Stratigraphic histogram of the Pinghu slope belt in the Xihu sag. Abbreviation: Sys.: System; Ser.: Series; Fm.: Formation; Mbr.: Member; Sg.: Sand Group; Sr.: Source rock; Rr.: Reservoir rock; Cr.: Caprock.

sedimentation occurred under marine regression settings, representing a semi-enclosed bay depositional environment in the marine-terrace transitional facies. Furthermore, hydrocarbon discoveries primarily occurred in the Pinghu Formation and Huagang Formation in the current stage of the Xihu Sag, with the Pinghu Formation also considered an important source rock interval within the sag (Wang et al., 2020; Zhu et al., 2012).

3. Materials and methods

3.1. Hydrocarbon migration and accumulation units (HAMU)

This study collected 10,273 km² of three-dimensional seismic

data from the slope belt and compiled well-logging data, geochemical survey data, fluorescence analysis, oil testing, and production data from 58 wells in the study area. According to comprehensive analyses of the petroleum geology of the Pinghu slope belt and the collected data, a mathematical model was established based on Hubbert's model (Hubbert, 1953) to determine seven HMAU in the Pinghu slope belt using hydrocarbon migration pathways and hydrocarbon supply ranges. The equation is presented as follows:

$$\emptyset = gz + \int_0^p \frac{\mathrm{d}p}{\rho} + \frac{v^2}{2} \tag{1}$$

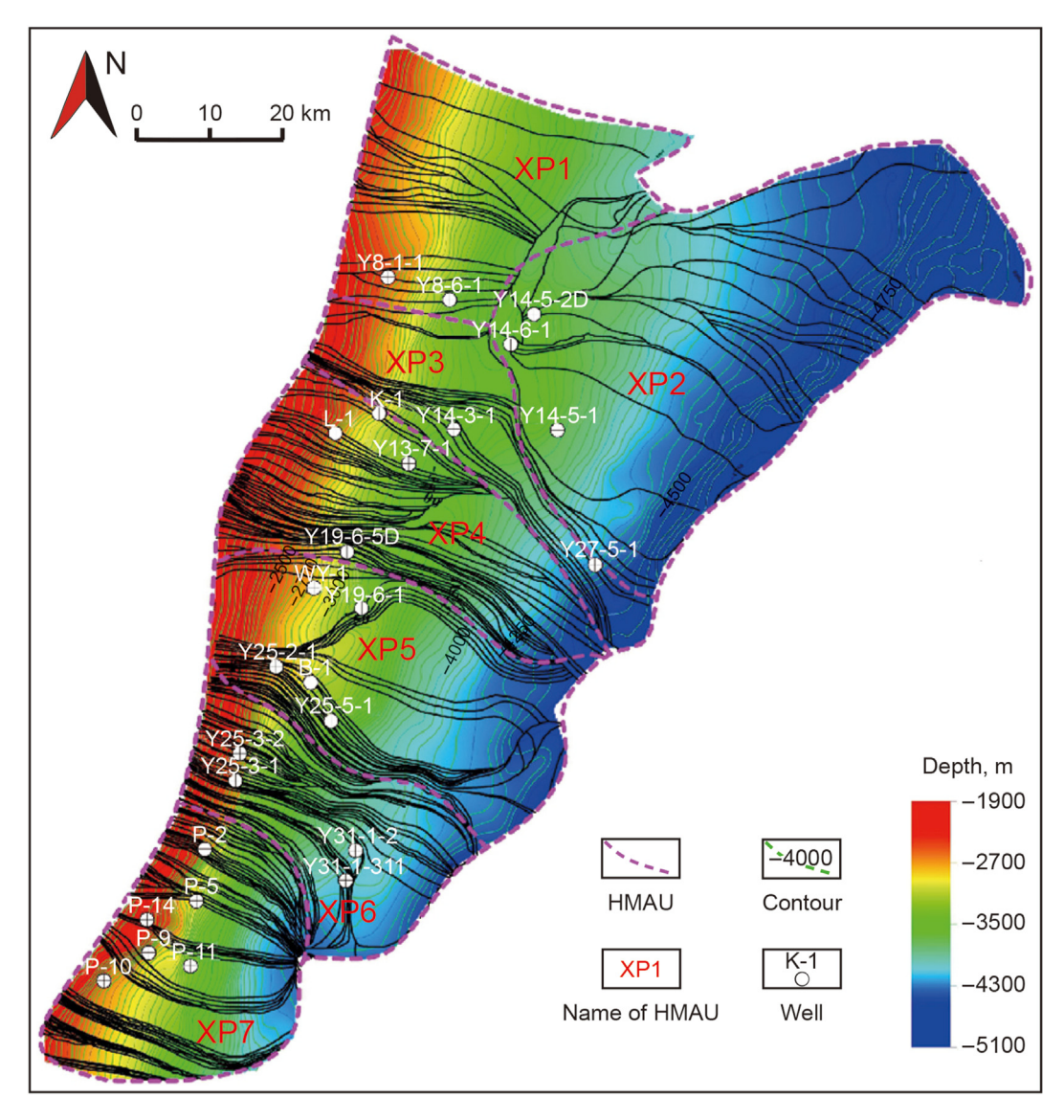


Fig. 3. Division of HMAU in the Pinghu slope belt.

where \emptyset is the fluid potential (J/kg), g is the gravity acceleration (m/ s²), z is the burial depth, p is the fluid pressure (Pa), ρ is the fluid density (kg/m³), and v is the flow velocity (m/s). The kinetic energy can be negligible due to minimal fluid velocity, v = 0.

The division of migration and accumulation units in this study is mainly based on the spatial distribution characteristics of sags and uplifts (Zhao et al., 2016), including the distribution of uplifts, slopes, and sags, structural morphology characteristics, sourcereservoir-cap rock patterns, source rock distribution, and confirmation of hydrocarbon discoveries. The final result is the map of large-scale hydrocarbon migration pathways and the division of HMAU. Following the "stratification and differentiation" approach, this study hierarchically examines the hydrocarbon distribution patterns in the entire area. Hydrocarbon distribution characteristics are thoroughly examined by conducting detailed analyses of typical reservoirs in the slope belt and combining oil testing and production data. Based on the slope belt's structural features and hydrocarbon distribution characteristics, the classification of hydrocarbon accumulation systems was established to analyze the hydrocarbon accumulation processes in critical HMAU, identify the main controlling factors of hydrocarbon accumulation, summarize

the patterns and models of hydrocarbon accumulation in the study area. These findings aim to improve the understanding of hydrocarbon accumulation in the Pinghu slope belt of the Xihu Sag, providing theoretical guidance for future exploration in the area.

3.2. Total organic carbon analysis and Rock-Eval pyrolysis

Total organic carbon (TOC) contents were measured after the removal of the carbonate bond using a 50% concentration of phosphoric acid. The TOC analysis was performed for all samples using a Leco CS-230 analyzer. For pyrolysis analysis, a Rock-Eval 6 instrument was utilized to measure the quantity of free hydrocarbons (HCs) (S_1 : mg HC/g rock) and HCs generated during pyrolysis (S_2 : mg HC/g rock). Depending on the TOC content, pulverized samples (<200 mesh) ranging from 5 to 50 mg were gradually heated in an oxygen-depleted inert atmosphere. Rock-Eval parameter S_1 represents free hydrocarbon content, and S_2 quantifies the amount of hydrocarbons generated through thermal cracking. To assess these parameters, the rock samples were subjected to pyrolysis at a steady temperature of 300 °C for 3 min, facilitating the quantification of heavy hydrocarbons beyond C_7 and

generating the S_1 . The thermal regimen was incrementally escalated from 300 °C to 550 °C at a controlled heating rate of 25 °C per minute. This escalation allowed for the measurement of heavy hydrocarbons exceeding C_{40} , constituting the S_2 parameter as outlined by (Peters, 1986). The S_1 and S_2 values were used to calculate the hydrocarbon generation potential ($S_1 + S_2$), a crucial metric in understanding the reservoir's hydrocarbon-accumulation capacity (He et al., 2021; Zhang et al., 2021, 2022).

3.3. Carbon isotope and inclusion

The carbon isotope analysis of the organic matter in all samples was conducted in accordance with GB/T 18340.2–2010, titled "Organic Geochemical Analysis Method for Geological Samples-Part 2: Determination of Organic Carbon Stable Isotopic Component-Isotopic Mass Spectrometry". The Finnigan Delta Plus isotope mass spectrometer was employed for the analysis. In the process, samples were reacted with 3 M HCl to eliminate inorganic carbon and then analyzed by using an Element Isoprime isotope ratio mass spectrometer to determine the $\delta 13$ Corg. Calibration was conducted against the Vienna-Pee Dee Belemnite standard (V-PDB), ensuring that replicate analyses consistently exhibited variations within $\pm 0.05\%$.

For the inclusion analytical method, the procedure involved the initial preparation of collected samples for examination, including slicing and dual-side polishing to create thin sections containing fluid inclusions. The petrographic analysis of these fluid inclusions was conducted using a microscope equipped with reflected light-transmitted light and fluorescence capabilities. This analysis focused on determining the type, occurrence, and size characteristics of the fluid inclusions. The instrument used in the analysis was a Nikon 80I dual-channel fluorescence microscope with an

ultraviolet excitation wavelength range of 330—380 nm (Van den Kerkhof and Hein, 2001). This rigorous methodology ensures a comprehensive understanding of both the stable isotopic composition of organic matter and the characteristics of fluid inclusions in the studied samples.

4. Results

4.1. Division and results of HMAU

A hydrocarbon migration and accumulation unit is a group of genetically connected reservoirs and traps with shared characteristics of hydrocarbon generation, migration, and accumulation, along with effective hydrocarbon kitchens providing hydrocarbon sources (Liu and Gao, 2003; Liu et al., 2022; Yu et al., 2018). The entire Pinghu slope belt is a first-order structure unit of the Xihu Basin (Zhang et al., 2022). This study divided the slope belt into HMAU from hydrocarbon accumulation. Each unit, after division, roughly corresponds to a second-order structure unit and includes hydrocarbon source rock areas that provide hydrocarbons.

As a typical sag-uplift slope belt in the Xihu Basin (Jiang et al., 2022), the Pinghu slope belt, in combination with existing hydrocarbon discoveries and geochemical tracing results, confirms that the hydrocarbons migrate from sags to slopes, with the main migration period occurring from the Miocene to the present. Hydrocarbon accumulation occurs on the slopes (Diao et al., 2020; Ding et al., 2021). Hydrocarbons are predominantly accumulated in the Pinghu Formation, with a small amount in the Huagang and Baoshi Formations (Yu et al., 2022). Seven HMAU were identified in the entire Pinghu slope belt based on the following aspects: previous knowledge and fluid potential theory (Hubbert, 1953), an emphasis on the influence of slope belt structural morphology,

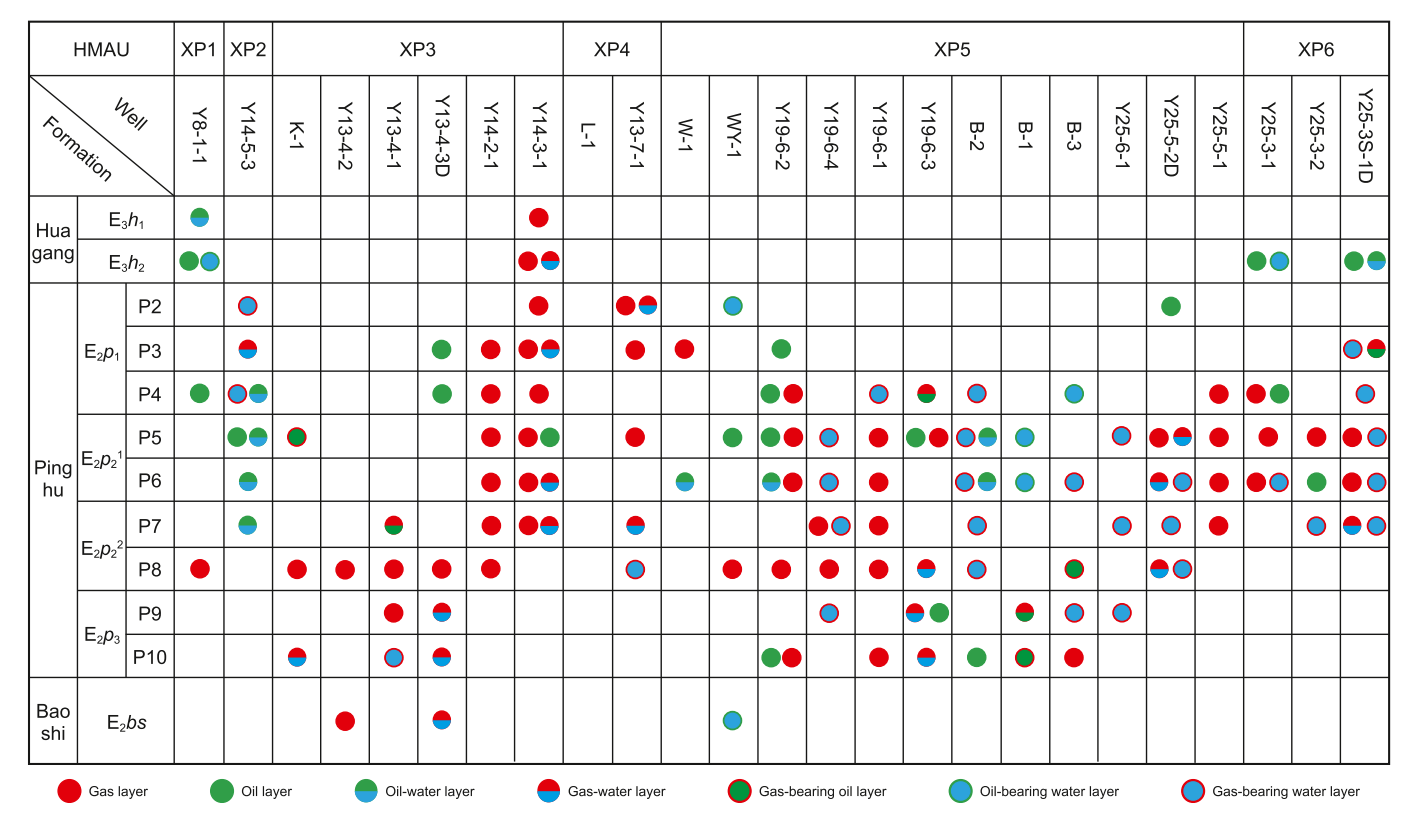


Fig. 4. Distribution of hydrocarbon reservoirs in the Pinghu slope belt. Abbreviations: HMAU: Hydrocarbon migration and accumulation unit.

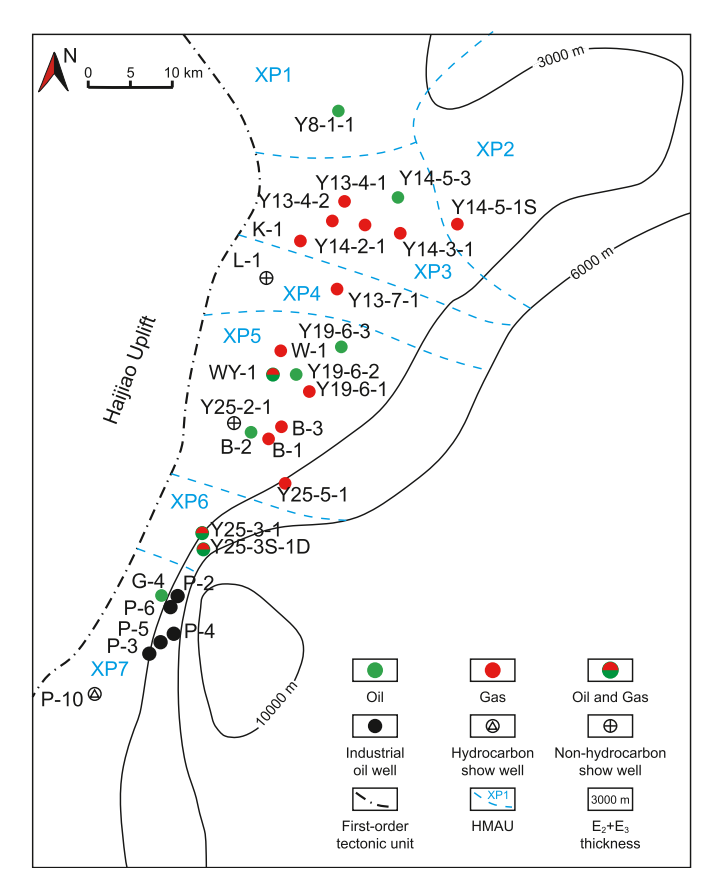


Fig. 5. Planar Distribution of hydrocarbon reservoirs in the Pinghu slope belt.

identified separation trough locations, determined migration pathways, analyses of the current state (primary hydrocarbon accumulation period), distributions of effective source rocks and source-reservoir-cap rock, reference to hydrocarbon discoveries from drilled wells, and structural morphology of the Pinghu Formation (represented by T3⁴ interface) in the slope belt. The HMAUs, labeled as XP1–XP7, are established with the objective of uncovering variations in hydrocarbon accumulation across distinct regions. However, this study did not investigate the XP7 unit due to a deficiency in relevant geological data (as illustrated in Fig. 3).

The hydrocarbon source of the XP1 unit comes from the northwest of the Y8 sag, and the hydrocarbons migrate westward after generation. The highest hydrocarbon shows are observed in well Y8-1-1, and well Y8-6-1 is located along the same migration route. Three migration pathways can be identified within the unit, with the dense northern and central pathways. However, the two wells indicating hydrocarbon shows are situated along the southern pathways, which show sparse pathways with parallel flow migration and moderate hydrocarbon supply conditions. The XP2 unit is primarily supplied with hydrocarbons from a portion of the Y8 and Y27 sags, ensuring abundant hydrocarbon sources. Overall, the unit possesses a "sag middle uplift" structure and favorable conditions for hydrocarbon accumulation. Hydrocarbon shows are observed at the highest position of the unit, and the pathways converge migration towards the high point, indicating excellent migration and accumulation conditions. The unit can be divided into two pathways: the northern and southern pathways. The northern pathway migrates towards Y14-5-2D and Y14-6-1 and extends further towards the west sag, covering a larger area of hydrocarbon accumulation. In addition, the southern pathway migrates towards Y14-5-1, with a smaller area of hydrocarbon

accumulation compared to the northern pathway. The XP3 unit receives hydrocarbon supply from two sources, the Y8 sag and the Y27 sag, ensuring abundant oil and gas sources. Hydrocarbon shows are observed in well K-1 at the highest slope position, indicating that the entire unit lies along an effective migration pathway. The primary migration pathway within the unit is located in the southern part, connecting the deep sag sources with slope belt traps and exhibiting dense pathways. In contrast, the northern part of the unit mainly receives hydrocarbon supply from the Y8 sag, resulting in sparse pathways and poor hydrocarbon supply. The XP4 unit is supplied with hydrocarbons from the Y27 sag, and hydrocarbon shows are observed in well Y13-7-1, but it is not located in a densely populated pathway area. The main migration pathways within the XP4 unit are located in the central part, extending from the sag towards the northwest before turning westward. The migration pathways are characterized by dense pathways and a large area of hydrocarbon accumulation, but the migration pathways in the southern and northern parts of the unit are sparse. The XP5 unit is supplied with hydrocarbons from the Y27 sag and contains an internal Y19 sag with abundant hydrocarbon sources. The main migration pathway within the unit is located in the northern part, with the pathways initially heading west-northwest before turning west-southwest, exhibiting dense pathway features with hydrocarbon accumulation. The southern pathways extend towards the west and northwest. However, significant blank areas without pathways occur within the unit, influenced by the structural morphology of the unit (distribution of internal uplift zones). The XP6 unit is supplied with hydrocarbons from the S36 sag, with a large area of hydrocarbon accumulation and a uniform distribution of migration pathways. Currently, hydrocarbon discoveries follow the distribution of pathways, with the highest hydrocarbon shows observed in well Y25-3-2, mainly consisting of oil. The XP7 unit is supplied with hydrocarbons from the S36 sag, with a large area of hydrocarbon accumulation and a uniform distribution of flow lines. The highest hydrocarbon shows are observed in well P-4, but wells P-10 and P-14 in the high zone exhibit poor hydrocarbon shows, which might be impacted by the hydrocarbon supply and migration conditions.

4.2. Characteristics of hydrocarbon distribution

The hydrocarbon distribution in the slope belt exhibits a pattern of "southern-northern sub-area division, eastern-western subbelt division, and variation in hydrocarbon accumulation". The hydrocarbon reservoirs are mainly distributed in the Pinghu Formation, followed by the Huagang Formation. The gas reservoirs in the Pinghu Formation are mainly produced gas condensate, while the oil reservoirs in the Huagang Formation are mainly composed of light oil. Overall, the hydrocarbons in the Pinghu slope belt are characterized by a predominance of gas over oil, with condensate as the primary component and crude oil as the secondary component. The planar distribution of hydrocarbon reservoirs exhibits "vertical stacking and lateral continuity", and hydrocarbon accumulation occurs in various types of traps at different zones. In the vertical direction, a multi-layer distribution of hydrocarbon exists in the slope belt, distributed in each member of the Pinghu Formation, showing a vertical distribution pattern of oil above gas. The hydrocarbon reservoirs are characterized by single sand layers or sand layer groups, with each sand layer (group) forming an oil-gas-water system unit. The thickness of hydrocarbon layers is generally less than 20 m, and the predominant type of reservoir is a layered reservoir with a water boundary.

The overall hydrocarbon distribution in the Pinghu slope belt exhibits characteristics of "southern-northern sub-area division and variation in hydrocarbon accumulation". For instance,

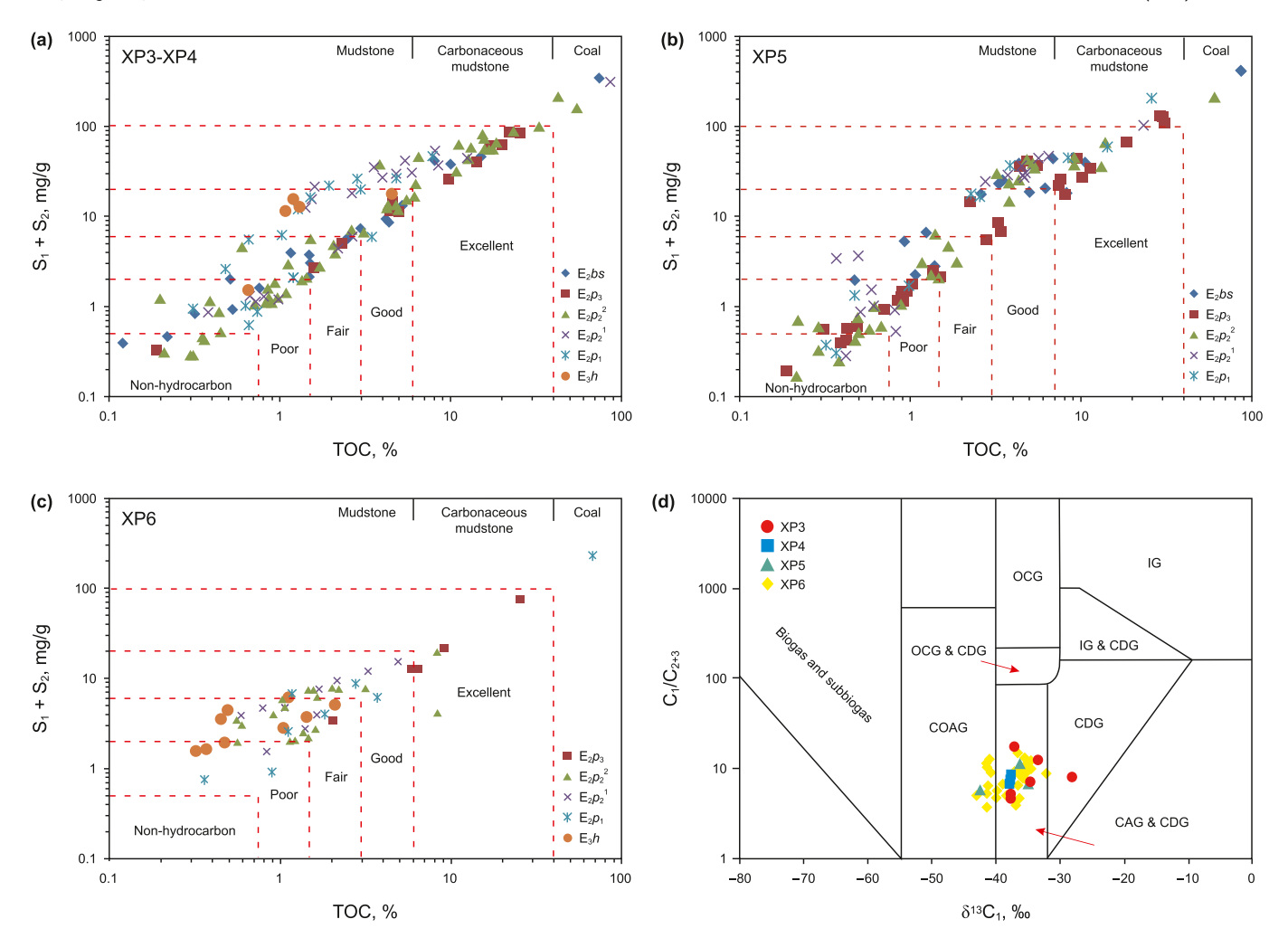


Fig. 6. (a) Correlation between Rock-Eval S_1+S_2 and total organic caron (TOC) in the Eocene-Oligocene of the XP3–XP4 units. (b) Variation of Rock-Eval S_1+S_2 with total organic caron (TOC) in the Eocene-Oligocene of the XP3–XP4 units in the Eocene-Oligocene of the XP5 unit. (c) Relationship between Rock-Eval S_1+S_2 with total organic caron (TOC) in the Eocene-Oligocene of the XP3–XP4 units in the Eocene-Oligocene of the XP6 unit. (d) Origin identification diagram of natural gas $\delta^{13}C_1$ -Lg(C_1 /(C_2 + C_3)) in the Eocene-Oligocene of the Pinghu slope belt. Abbreviations: Oil-cracking gas (OCG), Coal-derived gas (CDG), Crude oil-associated gas (COAG), Inorganic gas (IG), Condensate-associated gas (CAG).

hydrocarbons of the XP6 unit are distributed in the P4—P7 layers of the Pinghu Formation, while those of the XP5 unit are concentrated in the P6—P10 layers of the Pinghu Formation. The XP1—XP4 units are located in the synthetic fault terrace areas and correspond to the P3—P8 layers (Fig. 4). The planar distribution of hydrocarbon in the Pinghu slope belt exhibits certain macroscopic regularities. Specifically, the closer the distance to the hydrocarbon generation center in the deep sag, the higher the degree of gas accumulation. However, condensate content decreases in the condensate gas reservoirs, gradually transitioning to high oil-content condensate gas reservoirs towards the west. The horizontal and vertical distributions of oil-bearing zones vary in different areas (Fig. 5).

The XP3—XP4 units, located in the northern part, possess multiple hydrocarbon accumulation layers, and hydrocarbon shows have been observed from various layers of the Pinghu Formation, displaying a trend of accumulating near the sag. The number of hydrocarbon layers increases from the upper to the lower zones, and the reservoir layers become shallower at the same depth of hydrocarbon accumulation. The XP5 unit in the central part exhibits characteristics of hydrocarbon accumulation near the sag. In the lower part, the third fault trough area (wells Y19-6-1, Y19-6-2, and Y19-6-3) has significantly higher hydrocarbon abundance than the second fault trough area (wells W-1 and Y19-6-5D) and shows a

"mixed layer of oil and gas." For wells at the bottom of the fault trough, the hydrocarbon accumulation layers are located in the middle-lower to lower Ping Member of the Pinghu Formation, such as well Y19-6-1. In addition, the hydrocarbon accumulation layers of wells at the top of the fault trough are positioned in the middle-upper to upper Ping Member of the Pinghu Formation. The XP6 unit in the southern part shows an increase in the number of hydrocarbon layers from the upper fault terrace to the lower fault terrace (wells Y25-3-2 and Y25-3S-1D), and the hydrocarbon layers are mainly concentrated in the middle Ping Member (P5-P7) of the Pinghu Formation.

5. Discussion

5.1. Analysis of controlling factors for hydrocarbon accumulation in the slope belt

5.1.1. Analysis of variation in hydrocarbon distribution caused by hydrocarbon generation capacity and stratigraphy of source rocks and spatial configuration of source-slope

The organic matter abundance varies significantly in different structure units and intervals of the Pinghu Slope Belt. Three types of source rocks are primarily developed, including coal (TOC >40%),

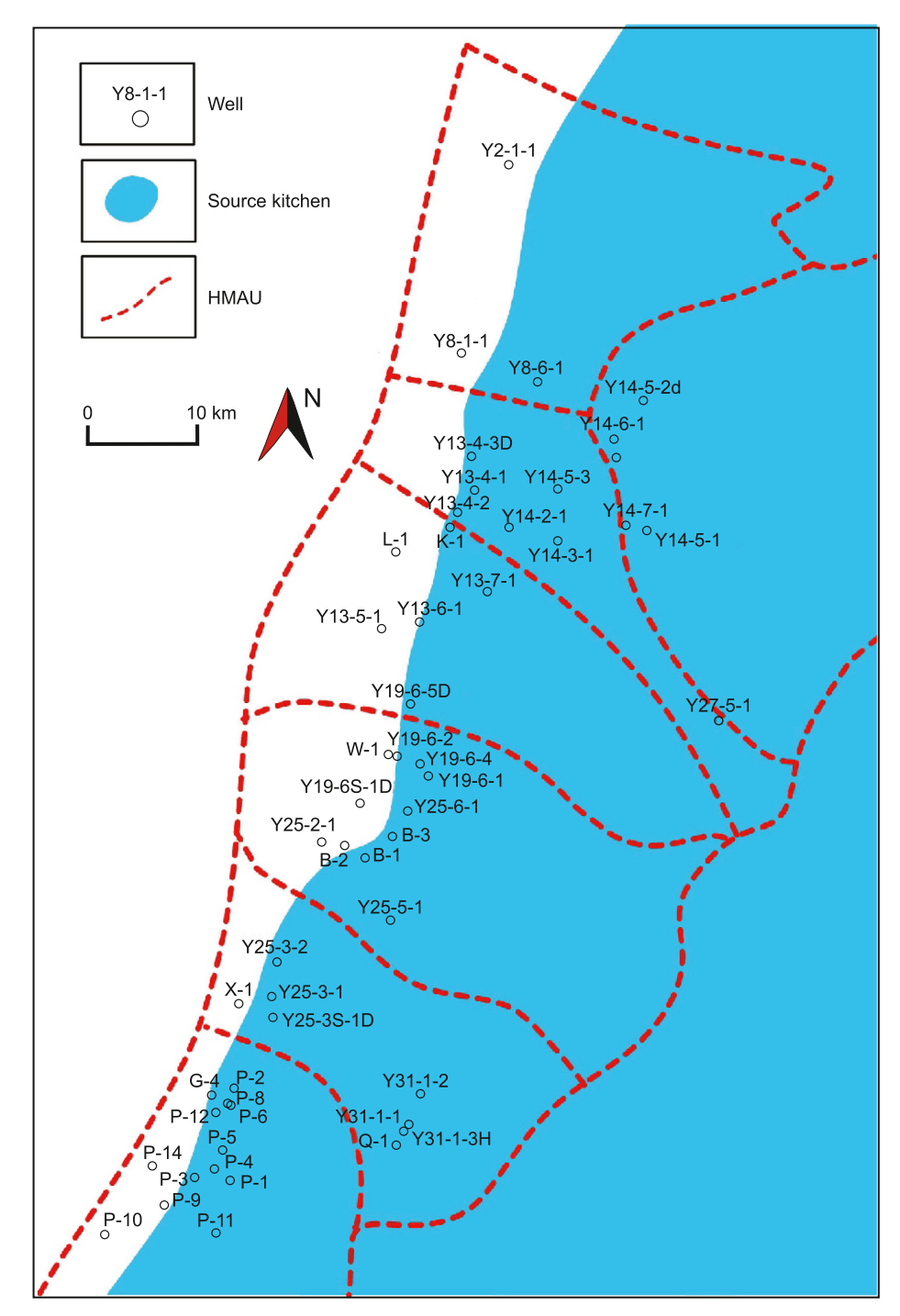


Fig. 7. Hydrocarbon kitchens range of source rocks in the Pinghu Formation of the Pinghu Slope Belt.

carbonaceous mudstone (6% \leq TOC <40%), and mudstone (TOC <6%) (Quan et al., 2022). From the relationship diagram of S_1+S_2 and TOC, the XP3-XP4 and XP5 units have higher hydrocarbon generation potential (as shown in Fig. 6a and b). In comparison, the XP6 unit has less coal and carbonaceous mudstone, exhibiting moderate hydrocarbon generation potential (Fig. 6c). Different types of source rocks in the Pinghu Formation and Baoshi Formation in the study area serve as potential source rocks. However, the maturity of shallow source rocks is relatively low. Thus, the crude oil primarily originates from the mature Baoshi Formation as well as coal and organic-rich mudstone in the lower Ping Member. The

maturity levels of light hydrocarbons and associated gas are relatively high, with the associated gas mainly being associated gas from condensate (Fig. 6d). Simulation experiments have revealed that the hydrocarbon expulsion threshold for coal is approximately 270 °C (corresponding to Ro = 0.54%), and mudstone source rocks, represented by Type II kerogen, possess similar hydrocarbon generation characteristics. Therefore, most of the source rocks in the study area can enter the hydrocarbon generation threshold when the maturity reaches Ro = 0.54%, which can be utilized to determine the approximate range of hydrocarbon kitchens (Fig. 7b). As depicted in Fig. 7b, the range of hydrocarbon kitchens in the study

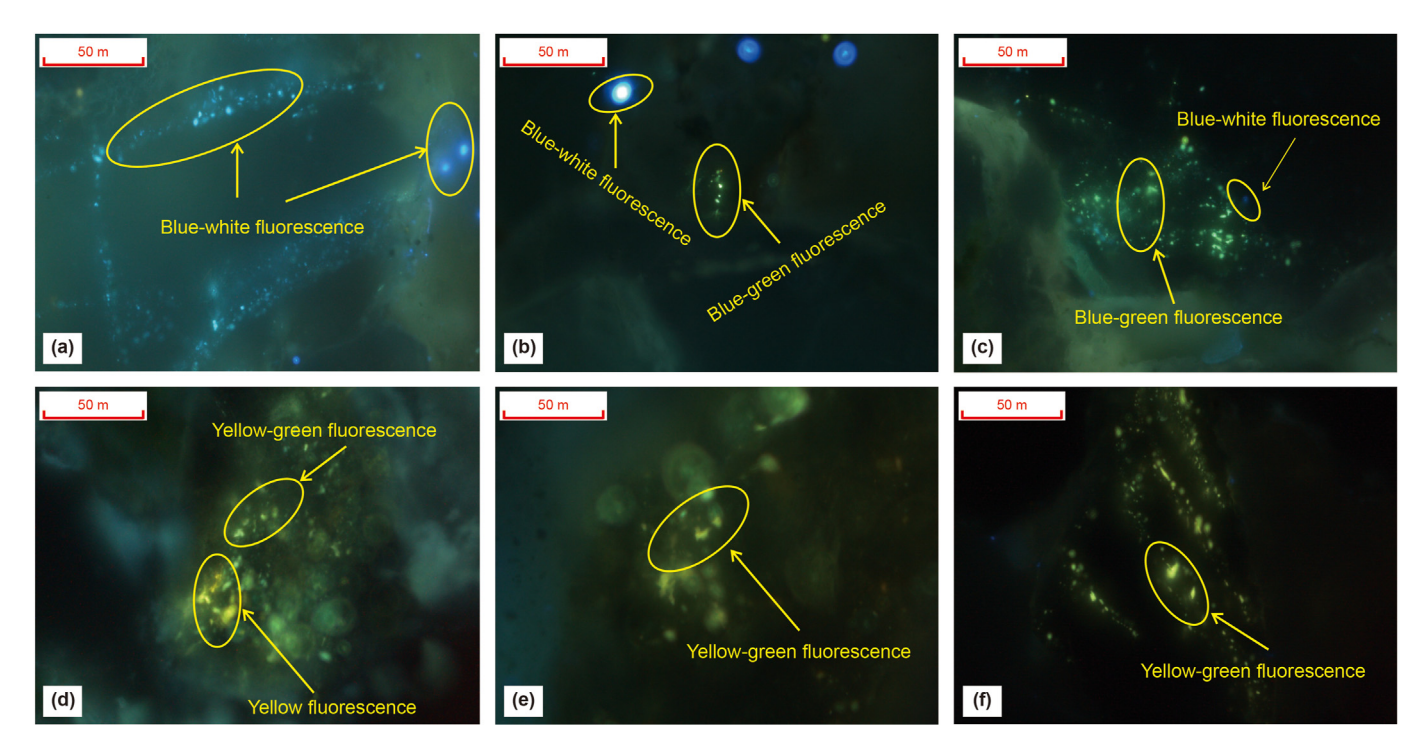


Fig. 8. Fluorescence microscopy images of petroleum inclusions in the Pinghu slope belt. **(a)** Wells Y8-1-1, 3,297 m, showing linear or layered distribution along cutting of quartz grain microfractures with blue-white fluorescence. **(b)** Wells Y14-7-1, 4,380 m, microfracture distribution after the diagenesis period along growth edge of quartz grains, displaying strong blue-white to weak blue-green fluorescence. **(c)** Wells Y19-6-4, 4,577 m, showing blue-green fluorescence within quartz grain cracks. **(d)** Wells Y19-6-5, 4,302 m, displaying yellow to yellow-green fluorescence within quartz grain cracks. **(e)** Wells Y19-6-5d, 3,614 m, microfracture distribution along cutting through quartz grains, exhibiting yellow-green fluorescence. **(f)** Wells Y19-6S-1dSa, 4,012 m, within microfractures along the cutting and growth edges of quartz grains, displaying yellow-green fluorescence.

area is extensive, covering a large area from the deep sag zone to the middle slope belt. Additionally, the regions possess a high intensity of hydrocarbon generation potential, providing favorable conditions for the hydrocarbon supply.

Fluorescence microscopy images of inclusions in the Pinghu slope belt reveal the presence of two types of petroleum inclusions: blue-green to blue-white colors (indicating high maturity, Fig. 8a, b, and 8c) and yellow to yellow-green colors (indicating low maturity, Fig. 8d, e, and 8f). The results demonstrate the occurrence of two periods of crude oil charge with different maturity levels in the study area, with the dominant lower-maturity oil charge in the early stage.

Statistical analysis of the homogenization temperatures of petroleum inclusions in the Pinghu slope belt reveals the existence of two distinct temperature ranges, which are 100-120 °C and 130-150 °C (Fig. 9a and b). Previous studies (Yang et al., 2019) on the hydrocarbon charge periods and paleo-pressure in the Pinghu slope belt have identified significant differences in the homogenization temperatures and trapping pressures of two types of petroleum inclusions: those exhibiting blue-green to blue-white fluorescence and those displaying yellow to yellow-green fluorescence. The first phase of hydrocarbon charge, represented by petroleum inclusions with orange-yellow to yellow fluorescence, has a homogenization temperature range of 101.9-122.1 °C and a trapping pressure range of 25.00-28.66 MPa. The second phase of hydrocarbon charge, represented by petroleum inclusions with blue-green to blue-white fluorescence, has a homogenization temperature range of 145.7–163.6 °C and a trapping pressure range of 38.60–44.31 MPa (Fig. 9c and d). Therefore, the Pinghu slope belt experienced two periods of hydrocarbon charge, with the first phase occurring during the early Miocene and the second phase spanning the middle to late Miocene until the present. This conclusion is confirmed by the findings of the study (Liu et al.,

2023).

Multiple hydrocarbon kitchens are developed in the central northern part of the XP1, XP2, XP3, and XP4 units, including the Y8 sag, Y19, and Y27. During the first phase of the hydrocarbon charge, the main oil supply comes from the local source rocks in the slope belt and sub-sag source rocks, and the crude oil undergoes shortdistance lateral migration. During the second phase of the hydrocarbon charge, the natural gas supply is mainly derived from the marginal source rocks of the deep sag zone (with higher maturity), and natural gas undergoes longer-distance lateral migration. Additionally, local and sub-sag source rocks can also contribute to some portion of the natural gas supply (with lower maturity). The Hydrocarbon charge is characterized by multi-phase and multihydrocarbon kitchens, resulting in the complex hydrocarbon distribution in the area. In the southern part of the XP4 unit and the northern part of the XP5 unit, the early-stage oil supply is mainly sourced from the vicinity of the Y19 sag, with the crude oil undergoing short-distance lateral migration. The later-stage natural gas supply is sourced from two different maturity hydrocarbon kitchens, the Y27 sag (primary source) and the Y19 sag (secondary source). For the Y27 sag, gas charge occurs in shallow layers (within and above the overpressure layer), characterized by heavy $\delta^{13}C_1$, high dryness coefficient, and high maturity (Ro approximately 1.4%). Natural gas charge in the Y19 sag occurs in deeper layers (below the overpressure layer), characterized by light $\delta 13C_1$, high humidity, and low maturity (Ro approximately 1.2%) (Fig. 10a). In the southern part of the XP5 unit, the hydrocarbon supply primarily comes from local source rocks and deep sag source rocks. Earlystage mature waxy crude oil charge undergoes near-source, and late-stage highly mature gas charge occurs from the deep sag zone, identifying as a combination of the two phases. The natural gas charge in the middle-low zone (well B-1 and well B-3) is significant, forming condensate gas reservoirs. In contrast, the gas charge in the

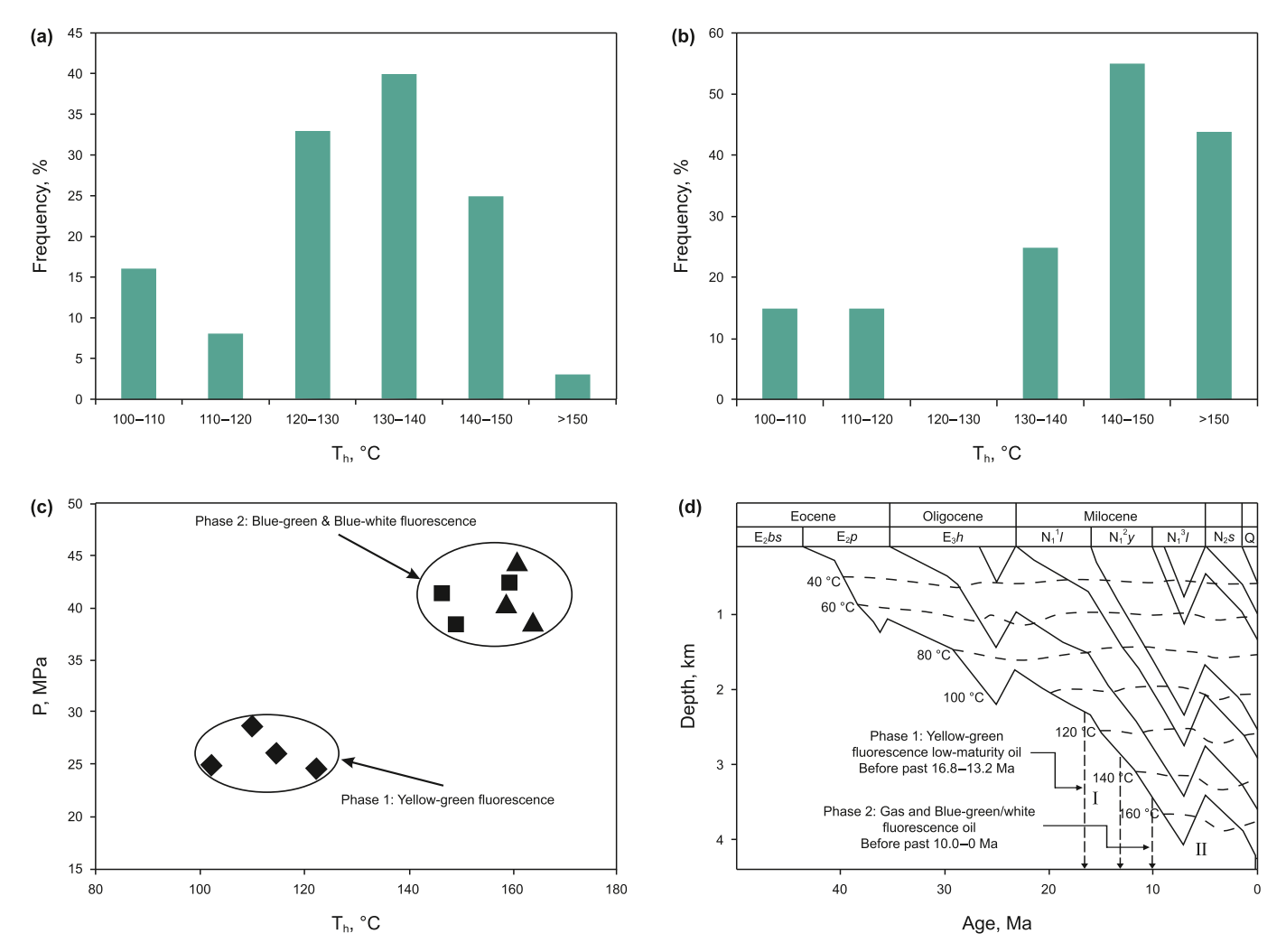


Fig. 9. Homogenization temperature statistics of petroleum inclusions in the Pinghu Formation of the Pinghu slope belt. (a) Wells Y19; (b) Wells Y25; (c) Distribution of trapping pressures and temperatures of two phases of petroleum inclusions in the Pinghu slope belt (Su et al., 2014); (d) Hydrocarbon charge history in the Pinghu Formation of the Pinghu slope belt (Su et al., 2014).

middle zone (B-2 well) is minor, preserving the characteristics of the original high-wax crude oil (Fig. 10b). In the XP6 and XP7 units, the hydrocarbon supply mainly comes from the S36 sag. Source rocks of the Pinghu Formation generate oil in the early stage and gas in the late stage. These hydrocarbons primarily migrate upward through major deep faults from the source rock layers. The early-formed oil reservoirs are subsequently modified by vertically migrating gas in the later stage (Fig. 10c, d, and 11c). The carbon isotope values of methane in natural gas display a decreasing trend from bottom to top, indicating a decrease in gas maturity from deep to shallow and suggesting vertical migration of natural gas.

The Pinghu slope belt contains abundant and high-quality source rocks distributed in the middle-upper, middle-lower, and lower Ping Members of the Pinghu Formation. Correspondingly, the hydrocarbon reservoirs are located in the upper, middle, and lower Ping Members of the Pinghu Formation. The distribution of hydrocarbon layers is controlled by the strata of the source rock. In the northern part of the Pinghu slope belt, the Y8 area has limited drilled wells, with only Wells Y8-6-1 and Y8-1-1, both primarily producing oil with little natural gas accumulation (XP1 hydrocarbon migration and accumulation unit has an estimated oil generation of approximately 30.1×10^8 t and gas generation of approximately 0.74×10^{12} m 3). The hydrocarbon accumulation in

the XP1 unit differs from all other HMAUs, and all these units also have hydrocarbon discoveries. Previous studies have focused on the geochemical characteristics of crude oil and comparisons with oil sources to determine the type and origin of oil in the XP1 hydrocarbon migration and accumulation unit (Li et al., 2022; Quan et al., 2022). However, few researchers have addressed the geological question regarding no or limited natural gas production in the Y8 sag of the XP1 hydrocarbon migration and accumulation unit (Liu et al., 2020). This study suggests that hydrocarbon supply conditions determine the differences in hydrocarbon distribution based on comprehensive analyses.

The primary hydrocarbon source rocks in the XP1 hydrocarbon migration and accumulation unit are located in the middle-lower Ping Member of the Pinghu Formation, comprising local source rocks and sub-sag source rocks (the Y8 sag). Although the local source rocks are extensively distributed in the unit, the sub-sag source rocks with a smaller distribution area dominate the hydrocarbon supply (Fig. 11a and b). The northern part of the slope belt (the XP1 and XP2 units) is more impacted by the NW-oriented structural transition zone, characterized by basin extension graben and fault-sag transition stages. Under weak transtension, the NNE-oriented faults gradually transform into sub-parallel SN-oriented and NNW-oriented faults, forming arc structures along the strike.

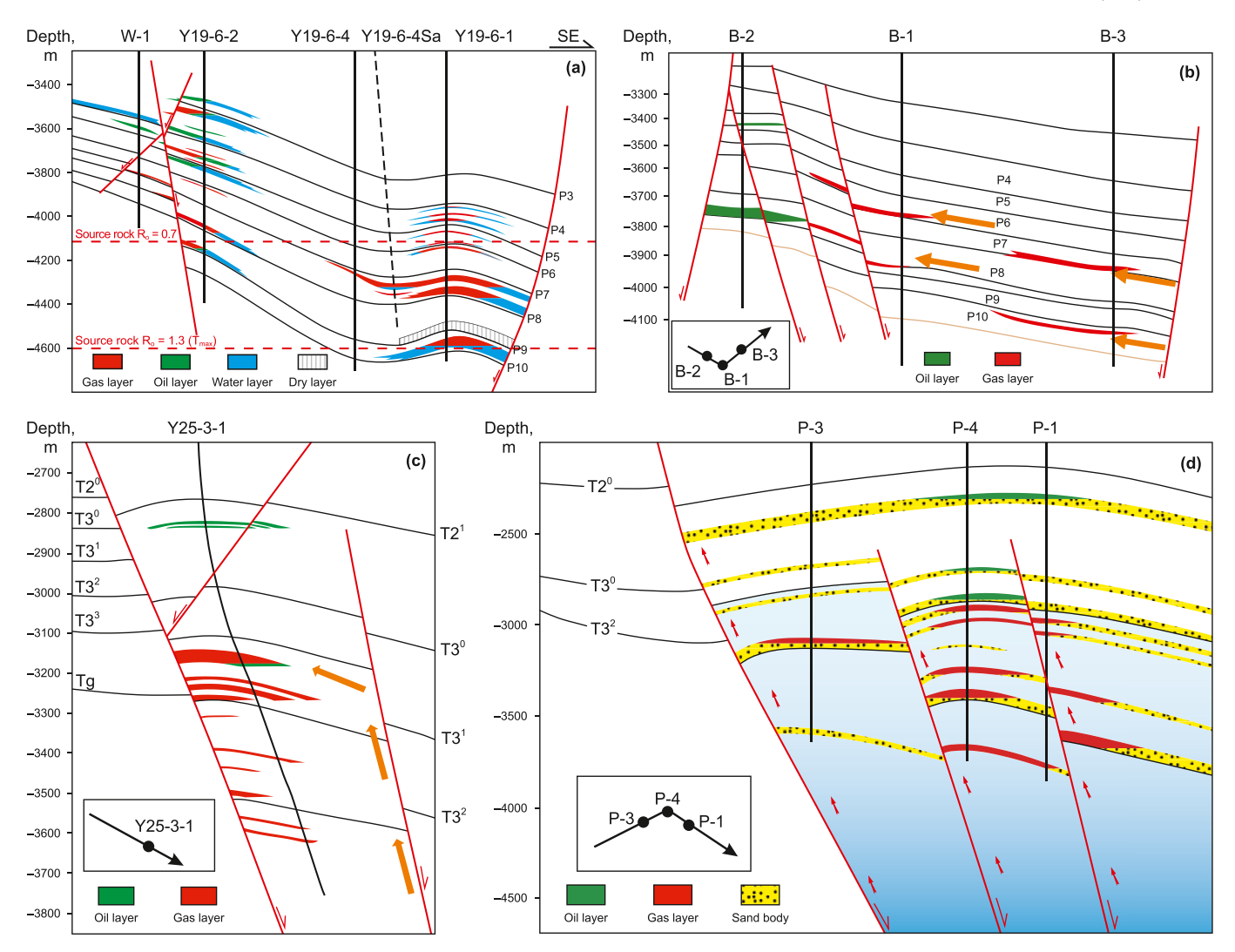


Fig. 10. Hydrocarbon migration pathways and accumulation patterns in the slope belt. (a) Central northern part of XP5 unit; (b) Central southern part of XP5 unit; (c) XP6 unit; (d) XP7 unit.

The HMAU and major migration pathways are noticeably controlled by structures. Ravines of the slope and saddles control the boundaries of HMAU, and low-amplitude structural ridges determine the hydrocarbon migration pathways. The XP1 and XP2 units are divided by the ridge of the arc structure (Fig. 11d), resulting in the XP1 unit only receiving hydrocarbons from the Y8 sag, where oil is predominantly generated. The natural gas generated in the deep sag of the XP2 unit is blocked by the structural ridge and cannot migrate to the XP1 unit, leading to an oil-dominated hydrocarbon accumulation in the XP1 unit without significant gas shows. This observation indicates that the differences in hydrocarbon accumulation between this unit and other units are closely related to the hydrocarbon generation capacity of source rocks, hydrocarbon supply types, and source-slope spatial configuration.

5.1.2. Differences in structural morphology, fault sealing capacity, and pressure induce variations in source-accumulation pathways

In the southern part of the XP6 unit in the slope belt, a set of NE-oriented deep main faults (PH faults) and their associated secondary faults developed during the initial rifting phase of the basin, characterized by long extension distance, large fault throw, and intense late-stage activity (Zhao et al., 2021). Numerous structural traps and structural-lithology composite traps are developed

around these deep main faults, formed before the hydrocarbon generation and expulsion period. These traps are located along the hydrocarbon migration pathways and serve as effective reservoirs, playing a significant role in hydrocarbon accumulation (Wang et al., 2021).

In the central and northern parts of the slope belt (the XP1–XP5 units), the influence of the NW-oriented structural transition zone is more prominent. During the extensional phase of the basin, NNE-oriented faults gradually transform from south to north into sub-parallel NS and NNW-oriented faults under the weak transtension, forming arc structures along the strike. Sediments from the higher areas converge along the NNW-oriented structural transition zone towards the lower sag. Under the impact of NNE-NS-NNW-oriented arc faults, fan-delta deposits gradually develop, controlled by the slope folding effect. Sand bodies are accumulated in the sag, favoring the development of high-quality reservoirs. Under the control of arc faults and NWW-oriented wrench faults, the main hydrocarbon source rocks in the deep sag and the hydrocarbons generated within the slope belt migrate along the NWoriented structural transition zone and the up-dip direction of the sand bodies. Hydrocarbon accumulation occurs due to the block of the faults with strong sealing capacity (Fig. 12). The NW-oriented structural transition zone is favorable for hydrocarbon

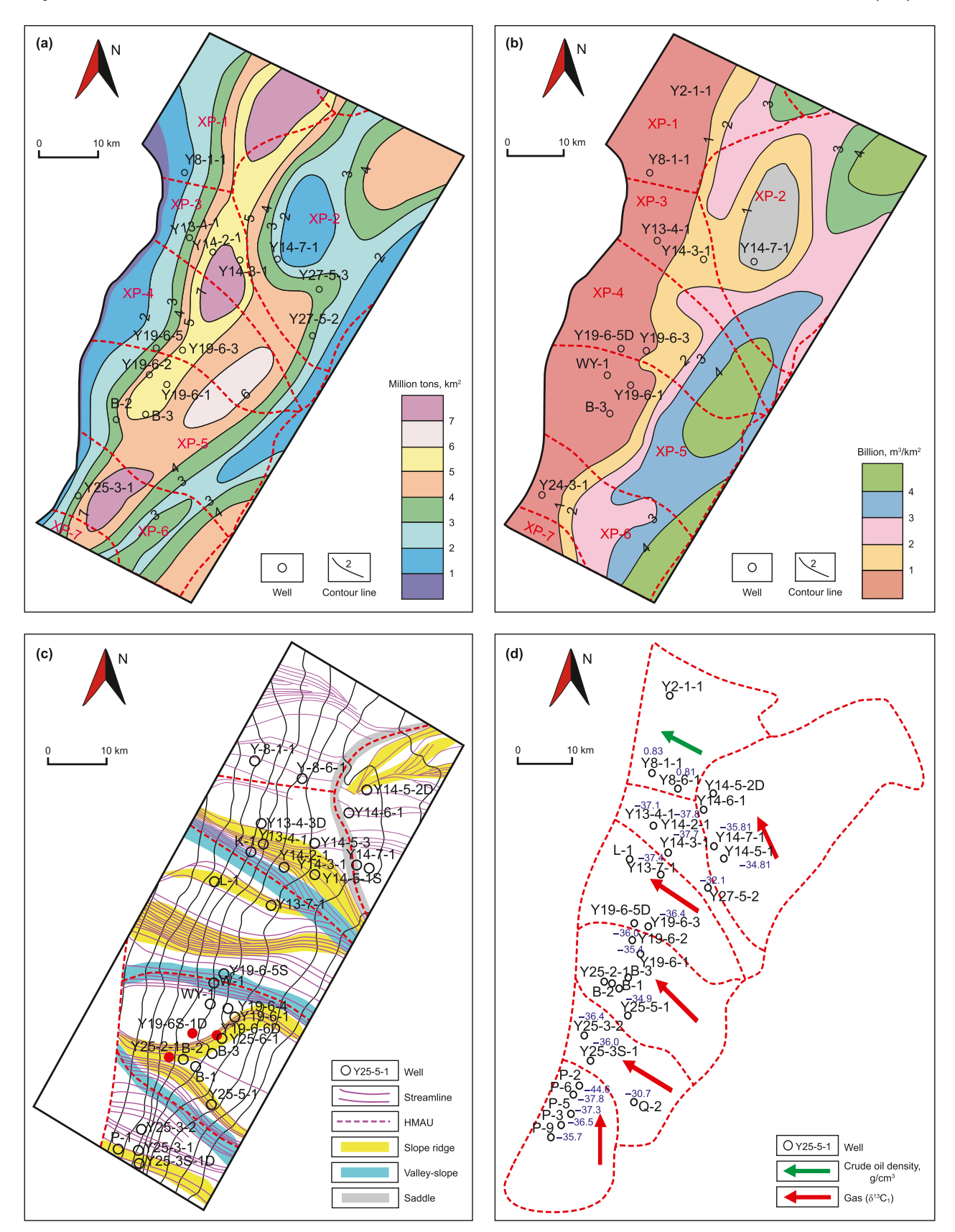


Fig. 11. (a) Oil generation intensity of the HMAU. (b) Gas generation intensity of the HMAU. (c) Migration pathways of HMAU in the slope belt. (d) Direction of hydrocarbon migration in the HMAU.

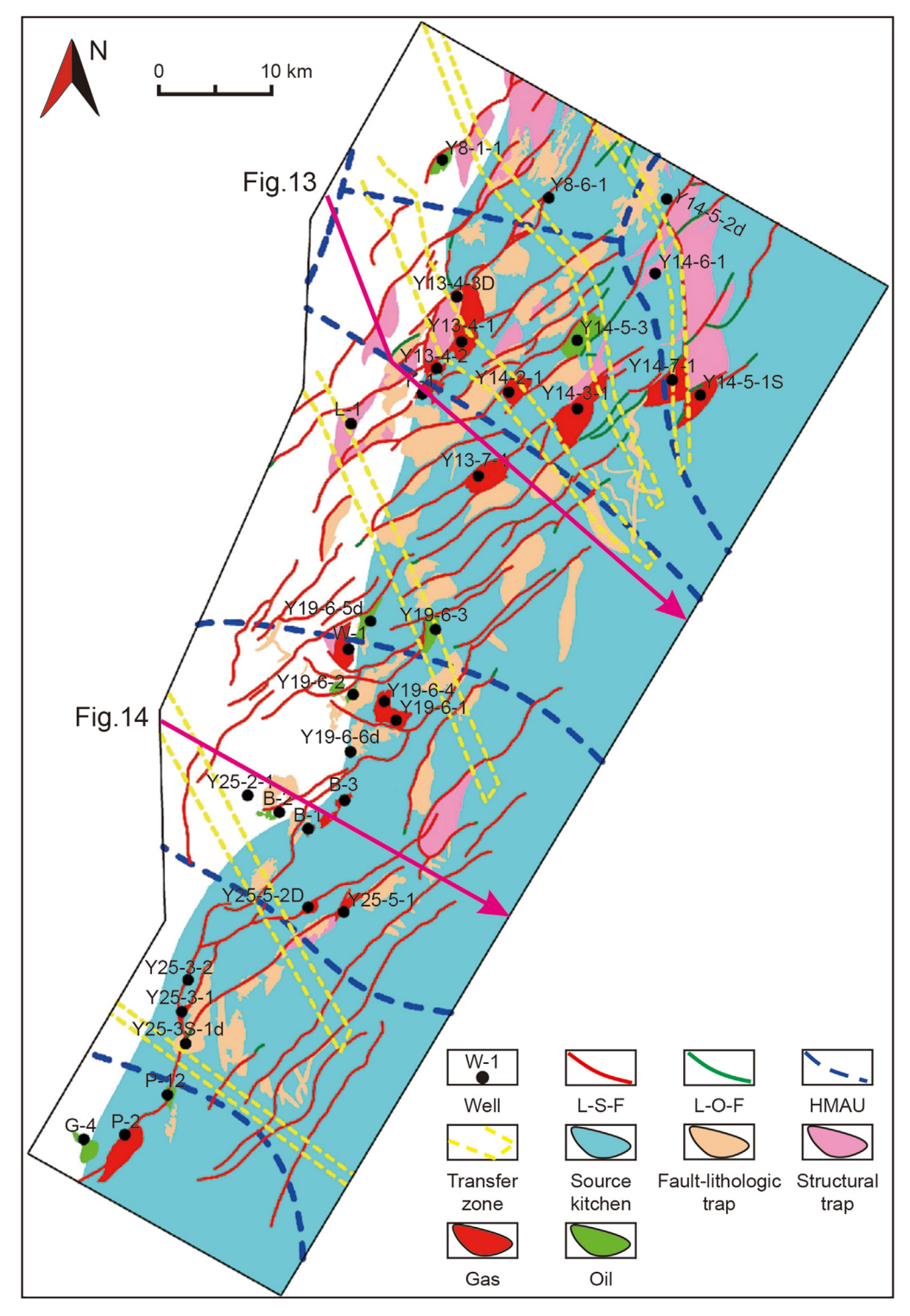


Fig. 12. Structural morphologies of the slope belt. Abbreviation: L-S-F: Lateral sealing fault; L-O-F: Lateral opening fault; HMAU: Hydrocarbon migration and accumulation unit.

accumulation, as observed in the southern XP3 unit and the northern XP5 unit. The XP3 unit is characterized by synthetic fault terraces, and secondary listric reverse faults develop in the lower slope belt (Fig. 13a and b). The XP5 unit is dominated by reverse fault troughs, with secondary reverse and normal fault terraces controlled by multiple reverse basement faults (Fig. 14a and b). The thickness of the Pinghu Formation is characterized by thine in the west and thick in the east. In addition, significant variations occur

in the source-accumulation pathways due to the different structural morphologies of the slope belt.

The fault sealing capacity (matched with cap rock) and pressure in the XP3 and XP5 units also differ. This investigation systematically compiles stratigraphic records, directly measured DST pressure data, corresponding log curves (acoustic curves and density logs), and mud logging data. These data are synthesized to construct regional pressure profiles for normal mudstone. The

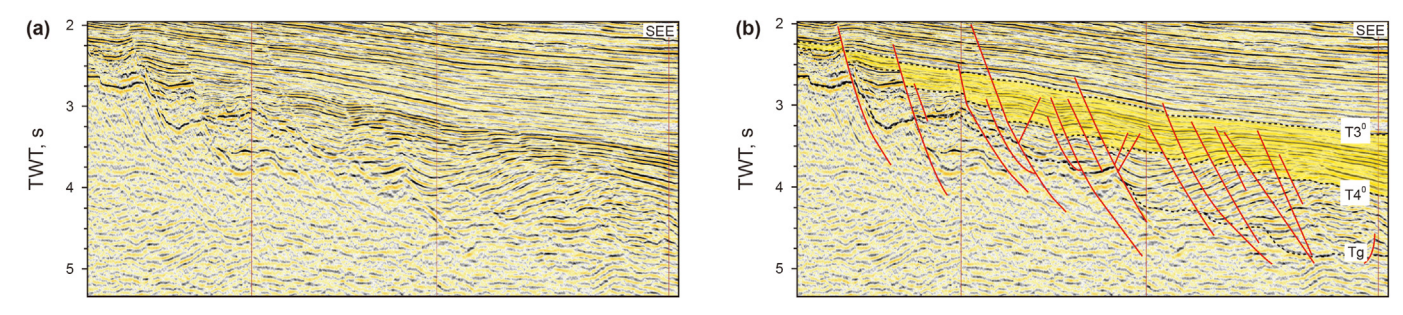


Fig. 13. Seismic profile characteristics of the XP3 Unit (location reference Fig. 12.).

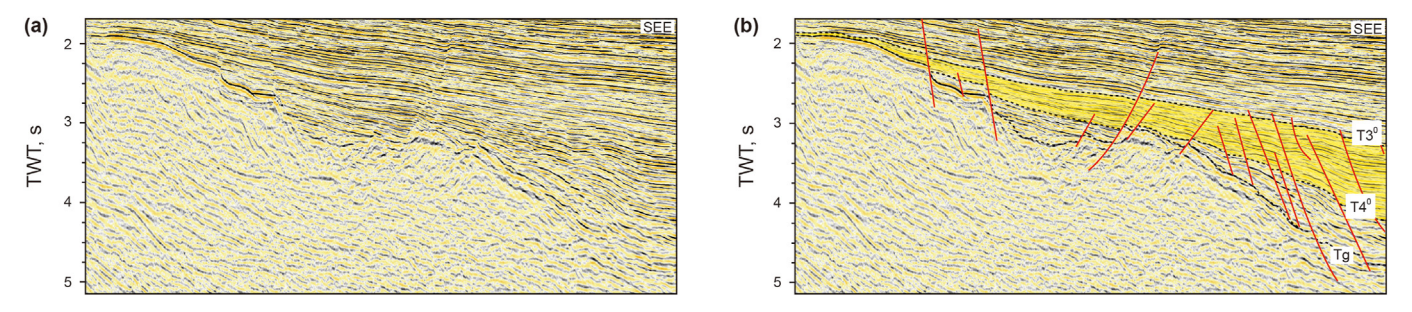


Fig. 14. Seismic profile characteristics of the XP5 Unit (location reference Fig. 12.).

research establishes that the acoustic curves of the Pinghu Formation adeptly reflect the formation pressures within the area. Consequently, these acoustic curves are coupled with density logs for pressure analysis and forecasting. Due to the high organic content in mudstones within overpressure zones, the acoustic transit times are anomalously high, complicating the accurate delineation of formation pressure characteristics. Leveraging insights from prior research (Li et al., 2021; Su et al., 2019), well log curves are meticulously adjusted for organic content based on the distribution of organic matter, depth of burial, and the actual acoustic curves.

The correlation between acoustic curves and rock density logs within the study area suggests that undercompaction significantly contributes to overpressure formation. Due to the substantial hydrocarbon generation potential within the Pinghu Formation, increments in overpressure resulting from hydrocarbon generation are noteworthy. Applying the EATON method (Eaton, 1972, 1976) using acoustic curves, formation overpressures are calculated and cross-validated with measured pressure readings (DST and mud weight pressures). Ultimately, a comprehensive overpressure distribution for the region is predicted and delineated, shedding light on the extensive variations in overpressure across the study area. In the XP3 unit, the middle-lower region develops local cap rocks in the Huagang Formation, and the middle-upper region forms local cap rocks in the Pinghu Formation. The local cap rocks from these two different strata juxtapose spatially and eventually develop into a regional cap rock (Fig. 15a). The presence of the regional cap rock leads to an increase in formation pressure in the XP3 unit. The pressure coefficient, as referenced from the research on overpressure distribution of the Pinghu Formation in the slope belt, gradually changes from 1.6 in the middle-lower region to 1.4 in the middle-upper region and finally to 1.0 in the upper region (Fig. 16a). Under the combined effects of overpressure and the regional cap rock, hydrocarbons in the lower region of the XP3 unit breakthrough fault sealing and migrate in a "cross fault and along fault" pattern. The hydrocarbons traverse multiple layers during migration while maintaining a consistent burial depth.

The regional cap rock of the P7 layer is primarily developed in the XP5 unit. Unlike the XP3 unit, the regional cap rock in the XP5 unit is not formed through the juxtaposition of multiple local cap rocks (Fig. 15b). Instead, the Pinghu Formation occurred a significant marine transgression during the sedimentation process of the Paleocene, resulting in the formation of approximately 180m thick black shale interbedded with thin sandy mud layers (Wu et al., 2017). This dense section of marine transgression shale (with mud content >40%) is an effective regional cap rock, increasing the probability of fault sealing during fault juxtaposition. The increase in formation pressure from the middle-lower to middle-upper regions in the XP5 unit occurs at a slower rate, with the pressure coefficient alteration from 1.3 to 1.1 (Fig. 16a). Due to the decrease in burial depth and the influence of sedimentary environments, the distribution range of open faults in the upper Ping Member of the Pinghu Formation is larger. Considering the greater burial depth and stronger diagenesis in the eastern part of the XP5 unit, it is predicted that lateral sealing appears in the upper Ping Member. Larger-scale faults of the shallow part in the upper Ping Member are more effectively sealed, while smaller-scale faults exhibit weaker sealing capacity. As a result, hydrocarbons migrate along fault planes in a "vertical bend" pattern (Fig. 16b). The observed differences in structural morphologies, fault sealing capacity (matched with cap rocks), and pressure lead to variations in sourceaccumulation pathways, ultimately resulting in variations in the vertical distribution of hydrocarbons.

5.1.3. Different fault-sand coupling patterns control the variation in hydrocarbon accumulation in various HMAU

The different synsedimentary fault combinations in the Pinghu Formation of the Xihu Sag are controlled by the tectonic stress field. Various fault combination patterns result in different types of structural transition zones, consequently controlling the variations in paleomorphology, leading to spatially distinct coupling patterns between sedimentary sand bodies and fault combinations (Fig. 17).

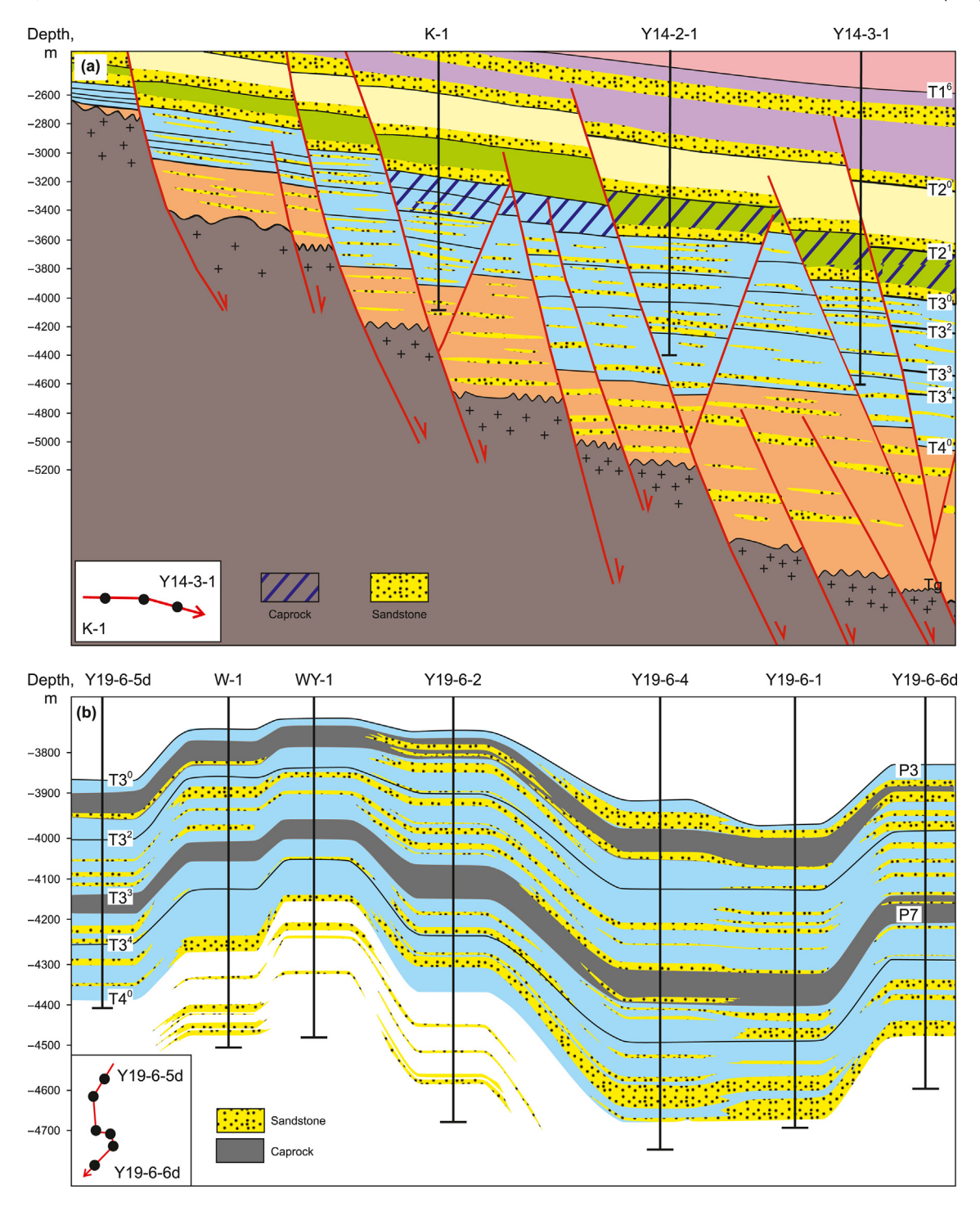


Fig. 15. Schematic of reservoir-cap rock of drilled wells in the Pinghu Slope Belt. (a) XP3 Unit; (b) XP5 Unit.

(1) The fault-sand coupling mode of the synthetic fault-terrace pattern mainly occurs within the XP1, XP2, and partial upper regions of the XP3 HMAU (e.g., the periphery of Wells Y13-4-2). NE- and NNE-oriented syn-sedimentary synthetic normal faults develop within these units, affecting the development location and extension of the terrestrial coarsegrained clastic systems and the depositional centers of sand bodies. Consequently, the delta-front subaqueous distributary channel sand bodies migrate along the bottom of the faults and accumulate in deep sag within the low-lying areas controlled by flexural topography, forming subaqueous distributary channel sedimentary sand bodies. These clastic sediments have coarse grain and significant thickness but a limited range of extension and distribution. The faults do not exhibit significant sand accumulation, making it challenging to form large-scale continuous reservoirs. The development area of these sedimentary sand bodies is generally adjacent to hydrocarbon-rich sag, with developed oil-source faults

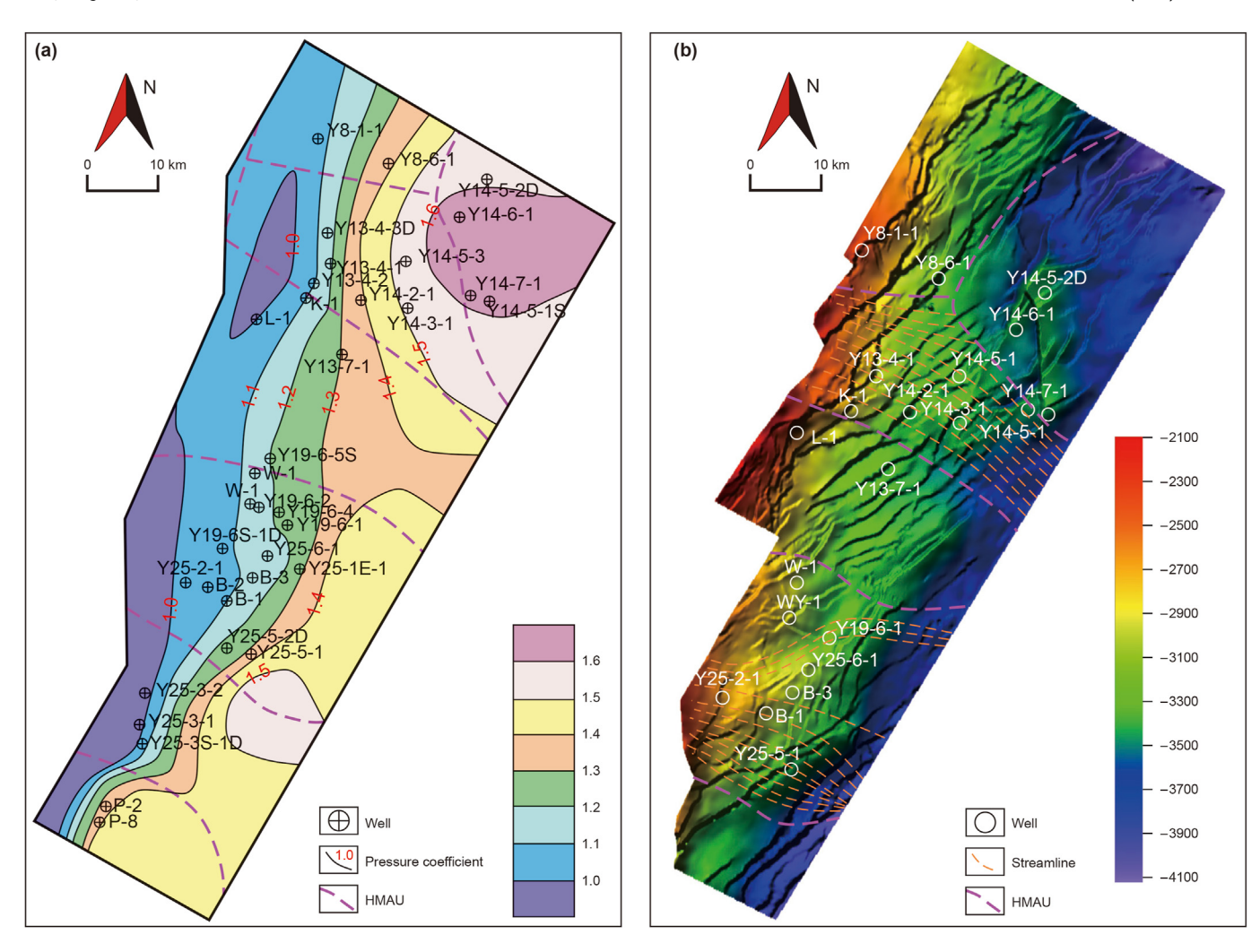


Fig. 16. (a) Schematic diagram of formation pressure distribution in the Pinghu slope belt. (b) Pathways distribution of the XP3 and XP5 Units.

- that can easily contact the hydrocarbon source rocks in subsags or deep sags. This phenomenon leads to the development of structural-lithological composite hydrocarbon reservoirs with superior reservoir-cap rock combinations and significant exploration potential (Fig. 17a).
- (2) The fault-sand coupling mode of the antithetic fault-terrace pattern mainly occurs in the southern part of the XP3 hydrocarbon migration and accumulation unit, within the middle-lower regions, as well as in the southern part of the XP6 unit. Extensive ravines develop within the western parts of these units under the sedimentary settings characterized by alternating sags and uplifts. These ravines are controlled by both synthetic and antithetic fault terraces. The bottom wall of the faults in the synthetic fault terrace stably subsides, gradually increasing the accommodation space for sediments. The antithetic fault-terrace zone plays a positive role in sand body accumulation. Sand bodies of the river channel are modified by the ravines and fault-terrace zones, ultimately achieving offloading sediments before the lowamplitude paleo-uplift at the basement. The paleotopography controls the lateral pinch of river delta channels influenced by tidal. In addition, fault sealing forms effective structural-lithological traps (Fig. 17b).
- (3) The fault-sand coupling mode of the en echelon division pattern mainly occurs in the peripheral area of Well Y13-7 within the XP4 hydrocarbon migration and accumulation unit. The superposition of NWW-SEE-oriented regional extensional stress and NE-SW-oriented weak extensional stress within this unit controls the formation of transition zones with en echelon pattern. These transition zones mainly possess two functions: (1) transporting water systems flowing from the upper region (e.g., near Wells L-1) and (2) locally aggregating sand, resulting in sand body accumulation at the low-lying of the bottom wall of synthetic normal faults and the development of compound sand bodies formed by subaqueous distributary channel sand and tidal sand bars. These sedimentary sand bodies have relatively coarse grain, considerable thickness, and extended lateral distance. The sedimentary sand bodies, coupled with hydrocarbon-rich sag and oil-source faults, form a variety of structural-lithological hydrocarbon reservoirs (Fig. 17c). Regions where the occurrence of this fault-sand coupling mode may become key areas for hydrocarbon exploration.
- (4) The fault-sand coupling mode of the half-graben sag trough pattern mainly occurs in the central-northern parts of the XP5 and XP6 HMAU. The middle-lower regions within the unit are characterized by graben structures. The bottom walls

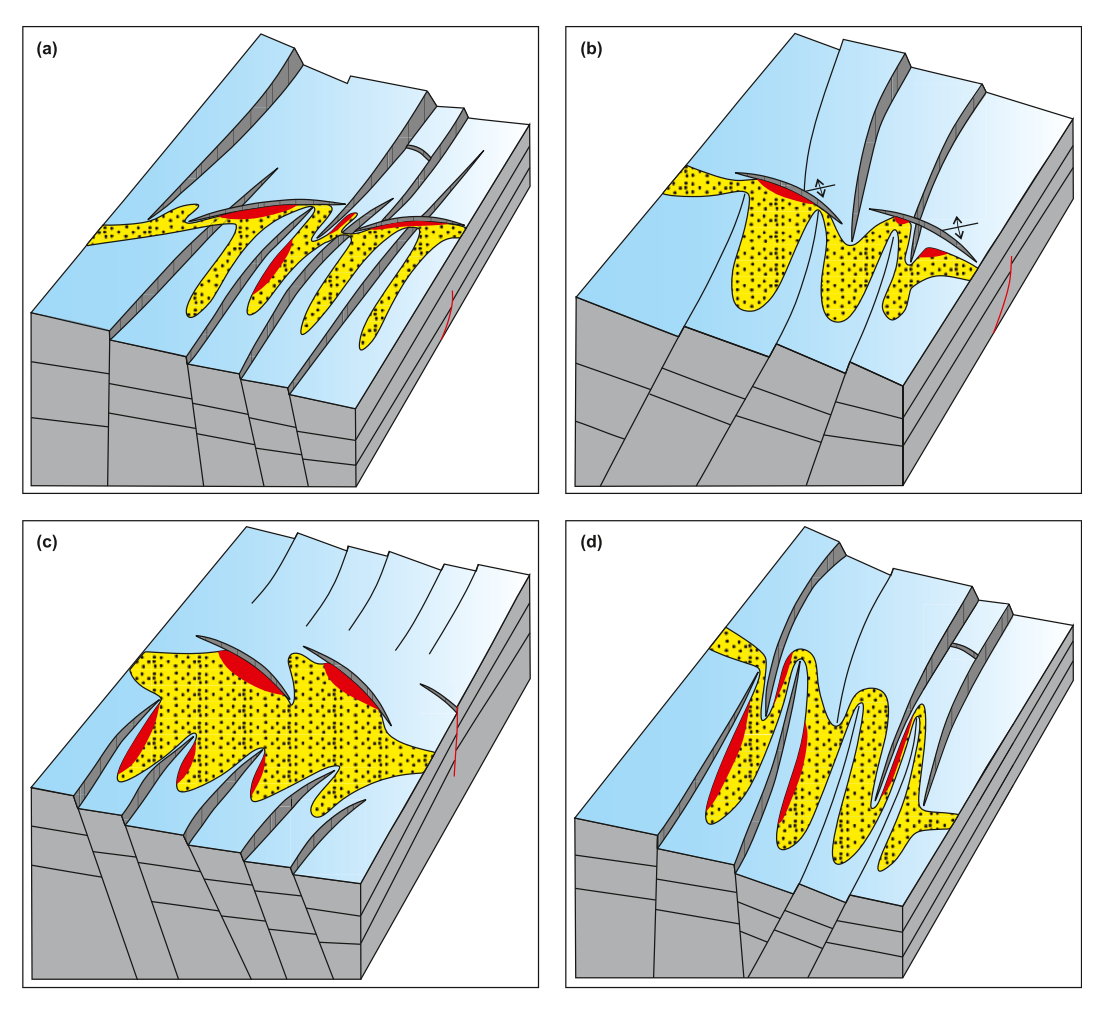


Fig. 17. Fault-sand coupling modes in the Pinghu Formation of the Pinghu Slope Belt. (a) Synthetic fault-terrace pattern, (b) antithetic fault-terrace pattern, (c) en echelon division pattern, (d) Basin-and-half-graben sag trough pattern.

of synthetic and antithetic faults cross and overlap, forming a water channel that transports paleowater systems along the low region and merging into the sag. The convergence capability of sand bodies depends mainly on the orientation and dip of the antithetic faults. Sand bodies and hydrocarbon accumulation tend to converge in the bottom wall of the antithetic faults, leading to the formation of structural hydrocarbon reservoirs and structural-lithological composite hydrocarbon reservoirs. The fault-sand coupling effect is significant, resulting in a high degree of hydrocarbon accumulation (Fig. 17d).

In a nutshell, the formation of structural-lithological hydrocarbon reservoirs is notably favorable within the synthetic fault-terrace pattern and the half-graben sag trough pattern, indicating a high potential for hydrocarbon accumulation. The en echelon division pattern, although influenced by multiple conditions, emerges as a promising focus for hydrocarbon exploration and may constitute a key area of interest. On the other hand, the antithetic fault-terrace pattern modified by the ravines and fault-terrace zones constrained by paleo-topography exhibits relatively smaller exploration potential compared to the other three models.

5.2. Hydrocarbon accumulation patterns in the slope belt

The Pinghu Formation of the Eocene in the slope belt develops

coal-bearing source rocks, abundant with crude oil from local nearsources as well as far-source sub-sag and deep sag overpressuredriven natural gas. The development of faults and structural transition zones creates "highways" (pathways) for hydrocarbon migration. Channel sands and tidal sand bars of the tidal-influenced delta front contribute to the formation of favorable reservoirs, facilitating the development of structural-lithological composite hydrocarbon reservoirs. The overall distribution of hydrocarbons in the slope belt exhibits a "vertical stacking and lateral continuity" pattern (Fig. 21). The distribution of oil and gas is intricately connected to the overpressure interface, with a prevalent tendency for oil reservoirs to be predominantly situated above the overpressure interface. In contrast, gas reservoirs are primarily located below it. This distribution pattern is influenced by the characteristic upward migration of gas, which occurs more readily than that of oil. The vertical distribution with oil positioned above gas in slope zone hydrocarbon fields can be attributed, in part, to the sequential nature of hydrocarbon migration and accumulation during the charging process. Furthermore, gas reservoirs require a more robust sealing capacity of the cap rock compared to oil reservoirs. In areas above the overpressure interface, lacking sufficient sealing pressure and regional cap rocks, gas fields encounter challenges in persisting. In contrast, below this interface, the sealing pressure effectively safeguards gas accumulations, significantly enhancing the possibility of gas reservoir formation. This phenomenon plays a pivotal role in shaping the distinctive oil-above-gas distribution

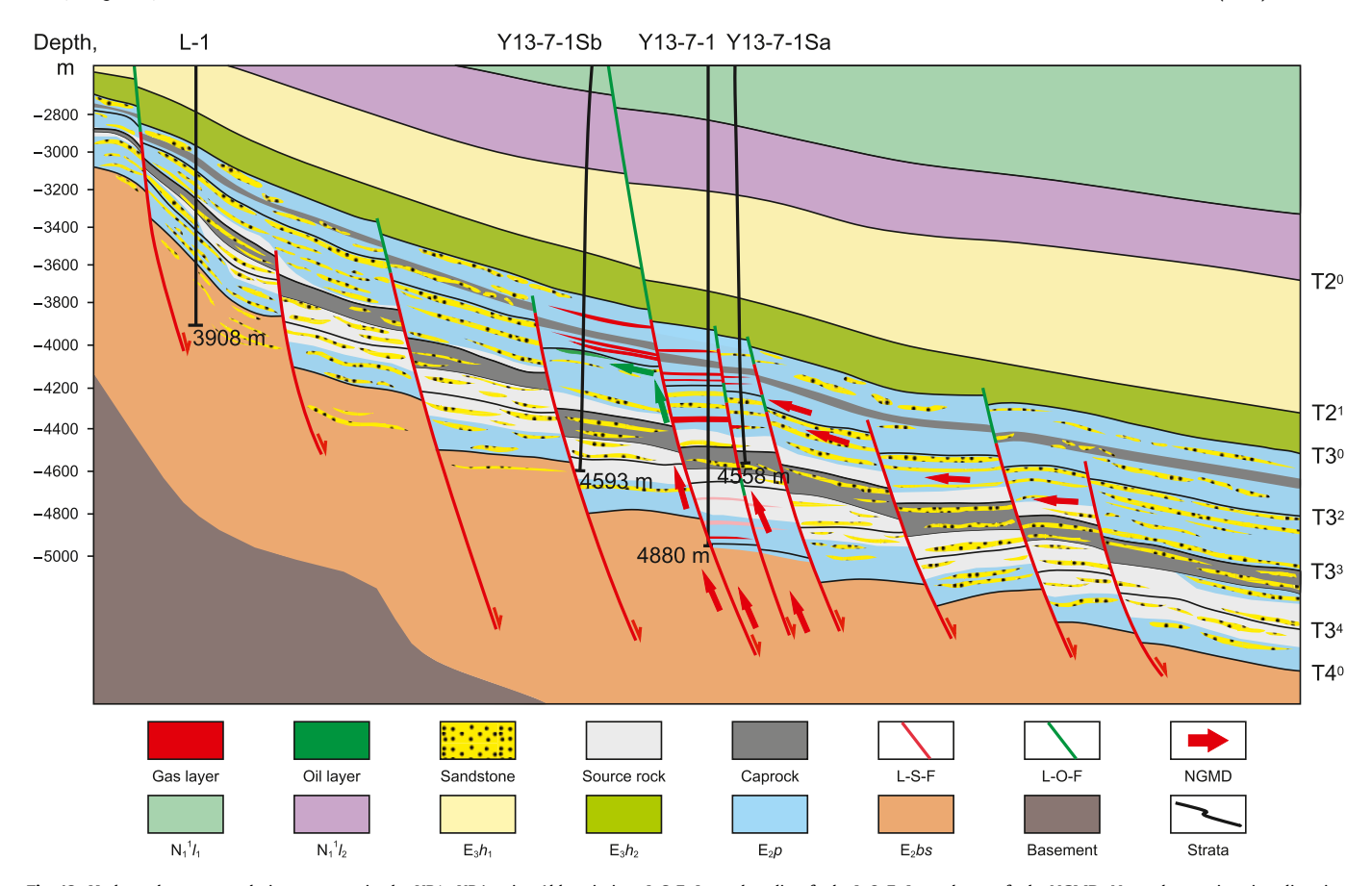


Fig. 18. Hydrocarbon accumulation patterns in the XP1-XP4 units. Abbreviation: L-S-F: Lateral sealing fault; L-O-F: Lateral open fault; NGMD: Natural gas migration direction.

pattern observed in hydrocarbon reservoirs.

5.2.1. Hydrocarbon accumulation pattern for near-source to farsource gentle slope with multiple hydrocarbon kitchens

The hydrocarbon accumulation pattern for near-source to farsource gentle slope with multiple hydrocarbon kitchens is established in the XP1-XP4 units. Tidal-influenced deltaic depositional systems are developed by controlling the synthetic fault-terrace characterized by western uplift and eastern tilt. The first phase of hydrocarbon charge primarily comes from the middle and lower regions of local near-source characterized by condensate and light oil, with short-distance lateral migration of crude oil. In the second phase of hydrocarbon charge in these units, the gas supply is primarily from the deep sag source rocks, with highly mature natural gas migrating over long lateral distances from sub-sags (the Y8 sag and the Y19 sag) or main sag (the Y27 sag). The deep sag exhibits a strong hydrocarbon supply capacity, ensuring continuously sufficient hydrocarbon charge. Within the XP1-XP4 units, a conspicuous increase in overpressure is evident when transitioning from elevated areas toward the depocenter. The region around the well L-1 high maintains normal pressure conditions. In the intermediate slope belt, represented by well Y13-7-1, the Pinghu Formation displays a pressure coefficient ranging from 1.2 to 1.3. Limited well data in the lower slope belt suggests a substantial overpressure in this area. The mudstone cap of the middle-lower Ping Member (P7) encounters challenges in vertical sealing due to fault-sand coupling, resulting in localized leakage. This leakage, occurring primarily at the lower part of the fault, results in the release of generated hydrocarbon and pressure. The outward release of pressure acts as a driving force for hydrocarbon migration. Consequently, oil and gas tend to migrate towards points of pressure release, facilitating the formation of hydrocarbon accumulations in the upper region. The hydrocarbon reservoirs generally exhibit weak overpressure characteristics. Fault blocks possess strong segmentation, leading to varying proportions of high-maturity gas mixing in the medium to lower regions. Late-stage hydrocarbon accumulation is characterized by the development of structural-lithological composite reservoirs, with the feature of "early oil and late gas, late-stage hydrocarbon accumulation" (Figs. 18 and 21b).

5.2.2. Hydrocarbon accumulation pattern for near-source to middle-source gentle slope with dual-hydrocarbon kitchens

The hydrocarbon accumulation pattern for near-source to middle-source gentle slope with dual-hydrocarbon kitchens is established in the XP5 unit. The XP5 unit forms hydrocarbon generation sub-sags and a series of antithetic fault troughs under the structural pattern of alternating sags and uplifts, developing a tidal-influenced deltaic depositional system. The first phase of hydrocarbon charge primarily comes from the near-source Y19 sag, with mature waxy crude oil undergoing short-distance lateral migration. In the second phase of hydrocarbon charge in the unit, the gas supply is mainly from the deep sag source rocks, with low-maturity natural gas originating from sub-sag (the Y19 sag) and highly mature natural gas migrating over longer lateral distances from the main sag (the Y27 sag). The charged natural gas is migrated through

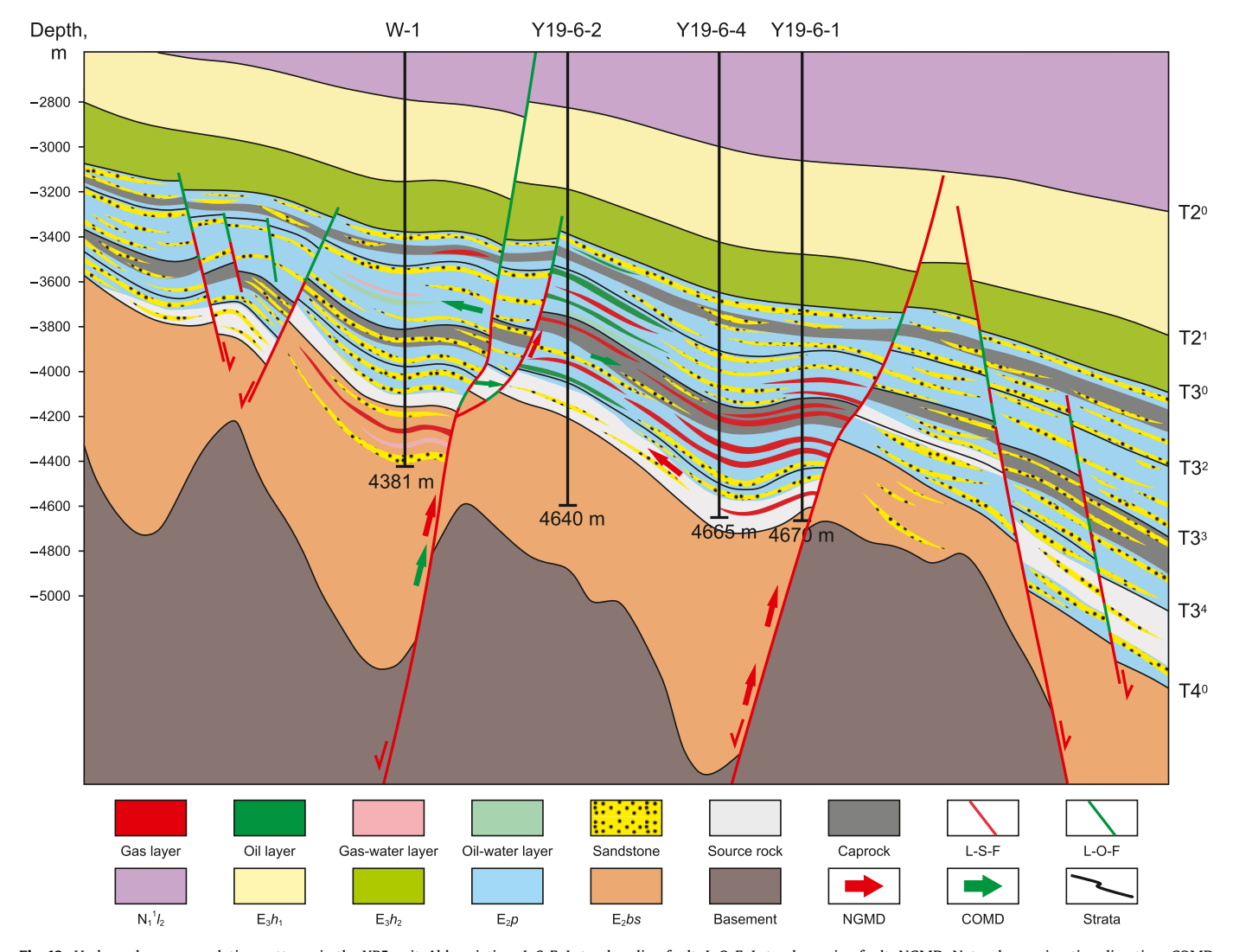


Fig. 19. Hydrocarbon accumulation patterns in the XP5 unit. Abbreviation: L-S-F: Lateral sealing fault; L-O-F: Lateral opening fault; NGMD: Natural gas migration direction; COMD: Crude oil migration direction.

the favorable pathways along the sand bodies in fault troughs, allowing the hydrocarbon to migrate and accumulate towards the upper region of the shallow layers within the overpressure system. Therefore, the XP5 unit has a strong hydrocarbon supply capacity and continuously sufficient hydrocarbon charge. The overpressure distribution in the XP5 unit reveals a distinct pattern of escalating intensity from the elevated regions of the slope to the deeper sections of the depression. The areas with the highest pressure levels are concentrated around wells B-3 and Y19-6-1, where the pressure coefficients exceed 1.4. Notably, within the broader slope region of XP5, the overpressure values in XP5 are comparatively restrained. This subdued overpressure is attributed to the probable limitations in connectivity within the current pressure system, leading to an uneven distribution of pressure structures. The formation of structural-lithological composite traps is controlled by sealed fault surfaces and sandstone pinches. In addition, the wellestablished fault-sand coupling relationship controls the charge intensity of dual-source hydrocarbons and the preferred direction

of hydrocarbon migration in the upper region (Figs. 19 and 21c).

5.2.3. Hydrocarbon accumulation pattern for near-source steep slope with a single hydrocarbon kitchen

The hydrocarbon accumulation pattern for near-source steep slope with a single hydrocarbon kitchen is established in the XP6 and XP7 units. The units are primarily controlled by the Pinghu major fault, forming a near-graben structural pattern. Under the setting of the steep slope of Pinghu major fault, tidal-controlled delta and tidal flats depositional systems are developed. Hydrocarbon is mainly supplied by the S36 sag, with early-stage oil generation followed by late-stage gas generation. The fault-sand coupling is well-established, providing favorable conditions for hydrocarbon migration and transport. Because antithetic faults are not developed, all faults are synthetic faults. The hydrocarbons mainly migrate to the upper part through faults from the source rock layer, given their proximity to the hydrocarbon kitchen. The overpressure distribution within the XP6—XP7 units exhibits a

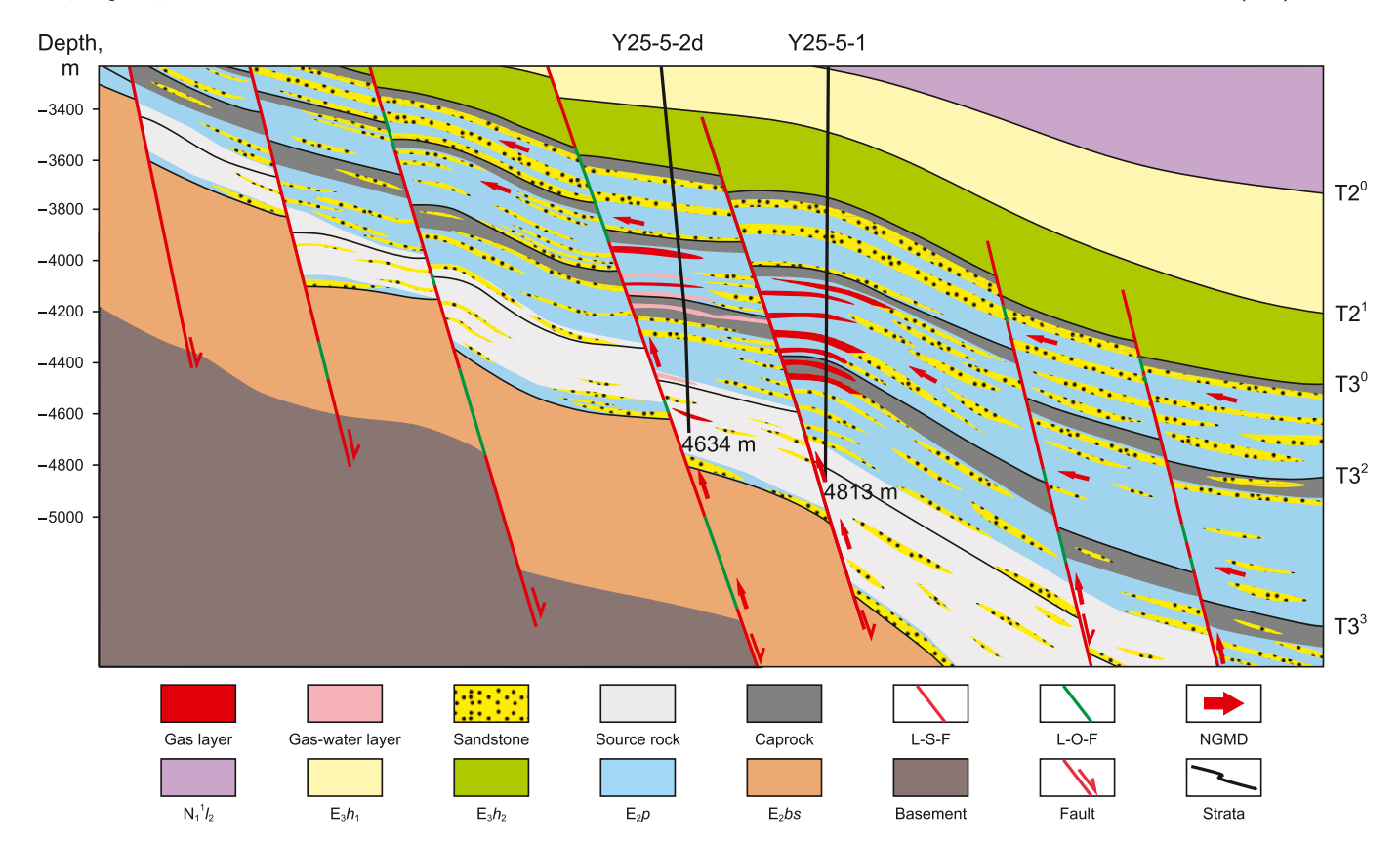


Fig. 20. Hydrocarbon accumulation patterns in the XP6-XP7 units. Abbreviation: L-S-F: Lateral sealing fault; L-O-F: Lateral opening fault; NGMD: Natural gas migration direction.

pronounced trend of incremental elevation from the elevated regions of the slope towards the basin depressions. The upper slope belt predominantly maintains normal pressure conditions, while the pressure coefficient increases to approximately 1.8 in the direction of the basin depressions. Microfractures, stemming from the overpressure, emerge as crucial pathways for the primary migration of hydrocarbon, facilitating episodic hydrocarbon expulsion. This residual pressure, a byproduct of the overpressure, plays a pivotal role as a driving force for the secondary migration of hydrocarbon. The spatial pattern of this residual pressure serves as a key indicator of both the dominant hydrocarbon migration pathways and the prospective regions for hydrocarbon concentration. Additionally, the development of structural traps and their superior quality leads to the hydrocarbon accumulation occurrence in multiple layers of the upper and lower sections (Figs. 20 and 21d).

6. Conclusion

1. Following the "stratification and differentiation" approach, migration and accumulation units were identified based on the spatial distribution characteristics of slopes, sags, and uplifts, as well as the structural morphologies features, hydrocarbon source-reservoir-cap rock patterns, the distribution of effective source rocks, and evidence of hydrocarbon discoveries. Through comparative analyses of the differences in hydrocarbon accumulation among different regions, seven distinct migration and

- accumulation units have been identified within the entire Pinghu slope belt, denoted as XP1–XP7.
- 2. The hydrocarbon distribution of the Pinghu Slope Belt in the Xihu Sag exhibits characteristics of "southern-northern subarea division, eastern-western sub-belt division, and variations in hydrocarbon accumulation". Deep major faults, structural transition zones, uplift settings, and regional cap rocks determine the hydrocarbon accumulation degree. Overall, the characteristics of hydrocarbons in the Pinghu slope belt are rich in gas and lean in oil, primarily condensate gas with high contents of condensate and following light crude oil.
- 3. In the Pinghu Slope Belt of the Xihu Sag, differentiated migration patterns have developed under the coupling settings of "structural features, sand body distribution, hydrocarbon generation capacity, and fault sealing capacity". This study reveals that source rocks control the hydrocarbon distribution, structural morphologies determine the direction of hydrocarbon migration, the spatial coupling between banded sand bodies and fault extension direction controls the development of structural-lithological reservoirs, and vertical and lateral sealing capacity of faults controls the hydrocarbon migration and accumulation. Significant differences exist between various migration and accumulation units.
- 4. Three hydrocarbon accumulation patterns have been established for the Pinghu Formation in the study area: near-source to far-source gentle slope with multiple hydrocarbon kitchens in the XP1–XP4 zones, near-source to middle-source gentle slope with dual-hydrocarbon kitchens in the XP5 zone, and

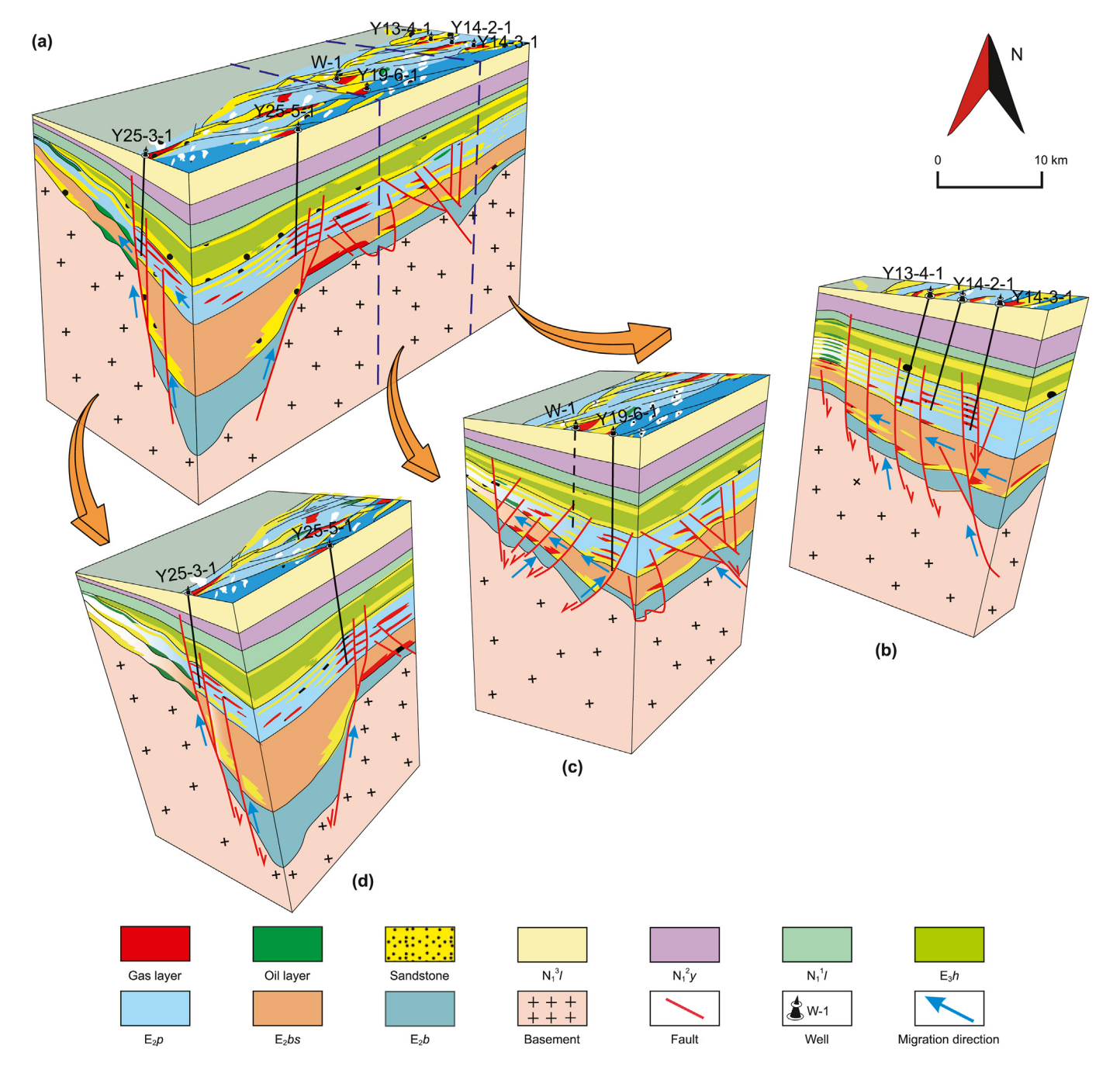


Fig. 21. 3D hydrocarbon accumulation patterns in the Pinghu slope belt. (a) 3D hydrocarbon accumulation patterns in the XP1–XP4 units, (b) 3D hydrocarbon accumulation patterns in the XP5 unit; (c) 3D hydrocarbon accumulation patterns in the XP6–XP7 units.

near-source steep slope with a single hydrocarbon kitchen in the XP6—XP7 zones.

CRediT authorship contribution statement

Bo Yan: Conceptualization, Formal analysis, Investigation, Methodology, Software, Validation, Visualization, Writing — original draft, Writing — review & editing. **Hong-Qi Yuan:** Conceptualization, Funding acquisition, Project administration, Resources, Supervision, Validation, Writing — review & editing. **Ning Li:** Funding acquisition, Resources, Supervision. **Wei Zou:** Funding acquisition, Project administration, Resources. **Peng Sun:**

Conceptualization, Funding acquisition, Supervision. **Meng Li:** Data curation, Visualization. **Yue-Yun Zhao:** Data curation, Software, Visualization. **Qian Zhao:** Visualization.

Declaration of competing interest

The authors declare that they have no known competing financial interests or personal relationships that could have appeared to influence the work reported in this paper.

Acknowledgment

This research was funded by the Natural Science Foundation of

Heilongjiang Province (LH 2022D013) and also supported by the Central Support Program for Young Talents in Local Universities in Heilongjiang Province (14011202101) and Key Research and Development Plan Project of Heilongjiang Province (JD22A022). The authors would like to thank the Research Institute of CNOOC Shanghai Branch, China, for their support in completing this study and permission to publish the results. Special thanks go to reviewers and editors for their insightful reviews and constructive suggestions to make the paper a better contribution.

References

- Abbas, A., Zhu, H.T., Zeng, Z.W., Zhou, X.H., 2018. Sedimentary facies analysis using sequence stratigraphy and seismic sedimentology in the Paleogene Pinghu Formation, Xihu depression, east China Sea Shelf basin. Mar. Petrol. Geol. 93, 287–297. https://doi.org/10.1016/j.marpetgeo.2018.03.017.
- Adeyilola, A., Zakharova, N., Liu, K.Q., Gentzis, T., Carvajal-Ortiz, H., Ocubalidet, S., Harrison, W.B., 2022. Hydrocarbon potential and organofacies of the devonian antrim shale, Michigan basin. Int. J. Coal Geol. 249, 103905. https://doi.org/ 10.1016/j.coal.2021.103905.
- Alves, T., Fetter, M., Busby, C., Gontijo, R., Cunha, T.A., Mattos, N.H., 2020. A tectonostratigraphic review of continental breakup on intraplate continental margins and its impact on resultant hydrocarbon systems. Mar. Petrol. Geol. 117, 104341. https://doi.org/10.1016/j.marpetgeo.2020.104341.
- Bailey, W.R., Underschultz, J., Dewhurst, D.N., Kovack, G., Mildren, S., Raven, M., 2006. Multi-disciplinary approach to fault and top seal appraisal; Pyrenees-Macedon oil and gas fields, Exmouth Sub-basin, Australian Northwest Shelf. Mar. Petrol. Geol. 23 (2), 241–259. https://doi.org/10.1016/j.marpetgeo.2005.08.004.
- Chabalala, V.P., Wagner, N., Malumbazo, N., Eble, C.F., 2020. Geochemistry and organic petrology of the permian whitehill formation, Karoo Basin (RSA) and the Devonian/Carboniferous shale of the Appalachian Basin (USA). Int. J. Coal Geol. 232, 103612. https://doi.org/10.1016/j.coal.2020.103612.
- Chen, Y.B., Cheng, X.G., Zhang, H., Li, C., Ma, Y., Wang, G., 2018. Fault characteristics and control on hydrocarbon accumulation of middle-shallow layers in the slope zone of Mahu sag, Junggar Basin, NW China. Petrol. Explor. Dev. 45 (6), 1050–1060. https://doi.org/10.1016/S1876-3804(18)30108-3.
- Chen, Z.Y., Du, X.B., Li, S., 2022. Distributional signatures of depositional system of Pinghu Formation, Pinghu slope, Xihu sag, east China Sea Shelf basin. Pet Geol Exp. 44 (5), 780–789. https://doi.org/10.11781/sysydz202205780 (in Chinese).
- Cumella, S.P., Woodruff, W.F., Revil, A., 2017. Piceance Basin Mesaverde anomalous self-potential response: identification of capillary seals in a basin-centered gas accumulation. AAPG Bull. 101 (1), 19—37. https://doi.org/10.1306/06201615130.
- Diao, H., Zou, W., Li, N., Qin, J., 2020. Hydrocarbon origin and reservoir forming model of wuyunting structure in Xihu depression, east China Sea Basin. Bull Geol Sci Technol 39 (3), 110–119. https://doi.org/10.19509/j.cnki.dzkq.2020.0312 (in Chinese).
- Ding, F., Liu, J.S., Jiang, Y.M., Zhao, H., Yu, Z., 2021. Source and migration direction of oil and gas in kongqueting area, Xihu sag, east China Sea Shelf basin. Mar. Geol. Quat. Geol. 41 (2), 156–165. https://doi.org/10.16562/j.cnki.0256-1492.2020090801 (in Chinese).
- Dong, D.W., Zhao, L., Li, T.T., Shi, R., Li, T., Sun, Y.F., Sun, H., 2019. Evolution mechanism and hydrocarbon reservoir characteristics of typical slope zones in Jizhong Depression, Bohai Bay Basin. Pet Geol Exp. 41 (4), 498–507. https://doi.org/10.11781/sysydz201904498 (in Chinese).
- Dong, Y.Q., Li, H.X., Wang, L., Liu, X.C., Wang, X.P., Li, N., 2014. Theory and methods of lithological reservoir exploration in qibei slope of qikou sag. Nat. Gas Geosci. 25 (10), 1630—1636. https://doi.org/10.11764/j.issn.1672-1926.2014.10.1630 (in Chinese).
- Eaton, B.A., 1972. The effect of overburden stress on geopressure prediction from well logs. J. Petrol. Technol. 24 (8), 929–934. https://doi.org/10.2118/3719-PA.
- Eaton, B.A., 1976. Graphical method predicts geopressures worldwide. World Oil 183 (1), 100–104. https://doi.org/10.1016/0038-092X(76)90080-3. Engelder, T., Lash, G.G., Uzcátegui, R.S., 2009. Joint sets that enhance production
- Engelder, T., Lash, G.G., Uzcátegui, R.S., 2009. Joint sets that enhance production from middle and upper devonian gas shales of the Appalachian Basin. AAPG Bull. 93 (7), 857–889. https://doi.org/10.1306/03230908032.
- Fan, T.L., Gao, Z.Q., Liu, C., Zeng, Q., 2008. The characteristics of Palaeozoic slopes with different geneses and oil/gas plays in the Tarim basin. Earth Sci. Front. 15 (2), 127–136. https://doi.org/10.3321/j.issn:1005-2321.2008.02.015 (in Chinese)
- Fei, B.S., 1999. Oil and gas exploration ingentle slope belt of dustpan sag. Multiple Oil-Gas Field. (03) 1–5. http://qikan.cqvip.com/Qikan/Article/Detail?id= 3766530
- Fu, X.F., Su, X.C., Gong, L., Wang, Q., Gao, S., Xie, Z., 2023. Control of faults and fractures on shale oil enrichment. Geoenergy Sci Eng 228, 212080. https://doi.org/10.1016/j.geoen.2023.212080.
- Fu, X.F., Wang, P.Y., Shen, J.N., Fu, G., Lv, Y.F., 2006. Oil and gas accumulation in simple slopes: a case study of the northern section of the western slope of Songliao Basin. Geol. Rev. (4), 522–531. https://doi.org/10.16509/j.georeview.2006.04.013 (in Chinese).
- Greb, S.F., Nelson, W.J., Elrick, S.D., 2020. Mining geology of the principal resource

- coals of the Illinois Basin. Int. J. Coal Geol. 232, 103589. https://doi.org/10.1016/j.coal.2020.103589.
- Guan, Y.W., Zhou, F., Pu, R.H., Fan, C.Y., 2022. Caprock characteristics and sealing evaluation of Pingbei gentle slope belt in Xihu Sag. Marine Geology Frontiers 38 (10), 34–41. https://doi.org/10.16028/j.1009-2722.2021.258 (in Chinese).
- He, W.T., Sun, Y.H., Shan, X.L., 2021. Organic matter evolution in pyrolysis experiments of oil shale under high pressure: guidance for in situ conversion of oil shale in the Songliao Basin. J. Anal. Appl. Pyrolysis 155, 105091. https://doi.org/10.1016/i.jaap.2021.105091.
- Hou, Y.C., Wang, H.Y., Fan, T.L., Yang, R., Wu, C., Tang, Y., 2019. Late syn-rift sequence architecture and sedimentary evolution of a continental rift basin: a case study from Fulongquan Depression of the Songliao Basin, northeast China. Mar. Petrol. Geol. 100, 341–357. https://doi.org/10.1016/j.marpetgeo.2018.11.029.
- Hu, C.Y., 1982. Source bed controls hydrocarbon habitat in continental basins, East China. Acta Pet. Sin. 3 (2), 9–13. https://doi.org/10.7623/syxb198202002 (in Chinese).
- Hu, J.Y., Xu, S.B., Tong, X.G., 1986. Formation and distribution of complex petroleum accumulation zones in Bohaiwan Basin. Petrol. Explor. Dev. 13 (1), 1–8 (in Chinese).
- Hu, M.Y., Li, S.Z., Dai, L.M., Suo, Y., Guo, L., Somerville, I., Liu, Z., Ma, F., 2018. Dynamic mechanism of tectonic inversion and implications for oil—gas accumulation in the Xihu Sag, East China Sea Shelf Basin: insights from numerical modelling. Geol. J. 53 (S1), 225–239. https://doi.org/10.1002/gj.3044.
- Hu, Y., He, W.X., Guo, B.C., 2020. Combining sedimentary forward modeling with sequential Gauss simulation for fine prediction of tight sandstone reservoir. Mar. Petrol. Geol. 112, 104044. https://doi.org/10.1016/j.marpetgeo.2019.104044.
- Hubbert, M.K., 1953. Entrapment of petroleum under hydrodynamic conditions. AAPG Bull. 37 (8), 1954–2026. https://10.1306/5ceadd61-16bb-11d7-8645000102c1865d
- Jia, C.Z., 2017. Breakthrough and significance of unconventional oil and gas to classical petroleum geology theory. Petrol. Explor. Dev. 44 (1), 1–10. https:// doi.org/10.1016/S1876-3804(17)30002-2.
- Jiang, D.H., Du, X.B., Li, K., Feng, Z., 2022. Distribution of sedimentary system multi-controlled by palaeo-geomorphology,water system and break during the deposition of Pinghu Formation,Baochu slope belt,Xihu Sag,East China Sea Shelf Basin. Pet Geol Exp. 44 (5), 771–779+789. https://doi.org/10.11781/sysydz202205771 (in Chinese).
- Jiang, Y.M., 2019. Detrital zircon U-Pb age and milankovitch cycles of Pinghu Formation in the Pinghu slope of Xihu depression: constraints on source-sink system and sedimentary evolution. Geol. Sci. Technol. Inf. 38 (6), 133–140. https://doi.org/10.19509/j.cnki.dzkq.2019.0615 (in Chinese).
- Jin, Z.J., Yun, J.B., Zhou, B., 2009. Types and characteristics of slope zones in Tarim Basin and their relationship with oil accumulation. Oil Gas Geol. 30 (2), 127–135. https://doi.org/10.11743/ogg20090201 (in Chinese).
- Kordi, M., 2019. Sedimentary basin analysis of the Neo-Tethys and its hydrocarbon systems in the Southern Zagros fold-thrust belt and foreland basin. Earth Sci. Rev. 191, 1–11. https://doi.org/10.1016/j.earscirev.2019.02.005.
- Lao, H.G., Wang, Y.S., Shan, Y.X., Hao, X.F., Li, Q., 2019. Hydrocarbon downward accumulation from an upper oil source to the oil reservoir below in an extensional basin: a case study of Chezhen Depression in the Bohai Bay Basin. Mar. Petrol. Geol. 103, 516–525. https://doi.org/10.1016/j.marpetgeo.2019.03.009.
- Li, G.X., Li, P., Liu, Y., Qiao, L., Ma, Y., Xu, J., Yang, Z., 2014. Sedimentary system response to the global sea level change in the East China Seas since the last glacial maximum. Earth Sci. Rev. 139, 390–405. https://doi.org/10.1016/ j.earscirev.2014.09.007.
- Li, H.C., Sheng, L.Q., Wang, Y.H., Xie, X., Jiang, X., Li, G., Wang, Y., Cheng, Y., 2001. Oil-gas exploration on slope. Oil Geophys. Prospect. 36 (5), 602–610. https://doi.org/10.3321/j.issn:1000-7210.2001.05.012 (in Chinese).
- Li, J., Zhao, J.Z., Hou, Z.Q., Zhang, S.P., Chen, M.N., 2021. Origins of overpressure in the central Xihu depression of the East China Sea shelf basin. AAPG Bull. 105 (No.8), 1627–1659. https://doi.org/10.1306/02262118112.
- Li, P.L., Zhang, S.W., Song, G.Q., Xiao, H.Q., Wang, Y.S., 2004. Forming mechanism of subtle oil pools in fault basins-taking the Jiyang depression of the Bohaiwan Basin as an example. Pet Geol Exp 26 (1), 3–10. https://doi.org/10.11781/sysydz200401003 (in Chinese).
- Li, S.X., Shao, L.Y., Liu, J.S., Qin, L.Z., Kang, S., Eriksson, K.A., Chen, X., Yu, Z., Liu, J., 2022. Oil generation model of the liptinite-rich coals: palaeogene in the Xihu sag, east China Sea Shelf basin. J. Petrol. Sci. Eng. 209, 109844. https://doi.org/10.1016/j.petrol.2021.109844.
- Li, W.H., Yang, E.Q., Wang, M., Huang, Y.R., 2022. Pore and fracture characteristics of Cretaceous tight reservoir and its control effect on hydrocarbon accumulation in the Liuhe Basin. Petrol. Sci. 19 (5), 1939–1949. https://doi.org/10.1016/ i.petsci.2022.06.015.
- Li, Y.J., Xu, F.B., Zeng, L.Y., Zhang, W.J., Li, M.L., Liao, Y.S., Chen, W.D., 2021. Gas source in lower Permian Maokou Formation and gas accumulation in the syncline area of eastern Sichuan basin. J. Petrol. Sci. Eng. 206, 109044. https://doi.org/10.1016/ j.petrol.2021.109044.
- Liang, J.T., Wang, H.L., Blum, M.J., Ji, X., 2020. Modeling of hydrocarbon migration and accumulation on the Chengzikou uplift, Bohai Bay Basin, China: implications for petroleum exploration on slope belts in rift basins. J. Petrol. Sci. Eng. 189, 106963. https://doi.org/10.1016/j.petrol.2020.106963.
- Liu, G.D., Gao, X.Z., 2003. Analysis of oil and gas migration and accumulation units: An effective way for oil and gas exploration and evaluation. Geol Sci. 38 (3), 307–314. https://doi.org/10.3321/j.issn:0563-5020.2003.03.004 (in Chinese).
- Liu, H.T., Yu, H.T., Sun, Y., Jiang, W., Yang, G., Wang, M., Wang, J., 2022. Formation

and differential enrichment of oil and gas on multiple types of slopes in rifted basins: taking the Bohai Bay Basin as an example, China. Acta Petrol. Sin. 38 (9), 2697–2708. https://doi.org/10.18654/1000-0569/2022.09.11 (in Chinese).

- Liu, J.Q., Wang, H.X., Lyu, Y.F., Sun, T.W., Zhang, M., He, W., Sun, Y., Zhang, T., Wang, C., Cao, L., 2018. Reservoir controlling differences between consequent faults and antithetic faults in slope area outside of source: a case study of the south-central Wenan slope of Jizhong Depression, Bohai Bay Basin, East China. Petrol. Explor. Dev. 45 (1), 88–98. https://doi.org/10.1016/S1876-3804(18) 30008-9
- Liu, J.S., Wei, Z., Li, N., Qin, J., Yang, L., 2019. Hydrocarbon accumulation control mechanism of reservoir-conservation coupling and its large and medium-sized fields exploration practice in Xihu sag,East China Sea basin. China Offshore Oil Gas 31 (3), 11–19 (in Chinese).
- Liu, J.S., Zhang, S.P., 2021. Natural gas migration and accumulation patterns in the central-north Xihu Sag, East China Sea Basin. Nat. Gas Geosci. 32 (8), 1163—1176. https://doi.org/10.11764/j.issn.1672-1926.2021.04.015 (in Chinese).
- Liu, L.L., Li, Y., Dong, H.Z., Sun, Z.Q., 2020. Diagenesis and reservoir quality of Paleocene tight sandstones, Lishui sag, east China Sea Shelf basin. J. Petrol. Sci. Eng. 195 107615. https://doi.org/10.1016/j.petrol.2020.107615.
- Liu, T.S., Ding, W.L., Yu, Z.W., Li, J., Wang, S., Zhou, X., Cheng, X., 2022. Characteristics of fluid potential and the division of hydrocarbon migration and accumulation units in the Nangong Sag, Bohai Bay Basin, China. Petrol. Sci. Technol. 40 (24), 2943—2959. https://doi.org/10.1080/10916466.2022.2052091.
- Liu, Y.Y., Fang, J.T., 1988. Preliminary study on formation conditions and enrichment degree of oil and gas pools in gentle slope zone of skip depression in Bohai Bay Basin. Petrol. Explor. Dev. (3), 21–26 (in Chinese).
- Liu, Y.Z., Zeng, J.H., Qiao, J.C., Chen, D., Li, S., Dong, Y., Liu, S.N., Long, H., 2023. Integration of charging time, migration pathways and sealing analysis to understand hydrocarbon accumulation in complex fault blocks, the Pinghu Slope Belt of the Xihu Depression, East China Sea Basin. Mar. Petrol. Geol. 152, 106241. https://doi.org/10.1016/j.marpetgeo.2023.106241.
- Luo, Q., 2010. Concept, principle, model and significance of the fault controlling hydrocarbon theory. Petrol. Explor. Dev. 37 (3), 316–324 (in Chinese).
- hydrocarbon theory. Petrol. Explor. Dev. 37 (3), 316–324 (in Chinese).

 Ma, C.F., Lin, C.Y., Dong, C.M., Elsworth, D., Wu, S., Wang, X., Sun, X., 2020. Determination of the critical flow pore diameter of shale caprock. Mar. Petrol. Geol. 112, 104042. https://doi.org/10.1016/j.marpetgeo.2019.104042.
- Martini, A.M., Walter, L.M., Budai, J.M., Ku, T.C.W., Kaiser, C.J., Schoell, M., 1998. Genetic and temporal relations between formation waters and biogenic methane: upper Devonian Antrim Shale, Michigan Basin, USA. Geochem. Cosmochim. Acta 62 (10), 1699—1720. https://doi.org/10.1016/S0016-7037(98) 00090-8.
- Meng, Q.A., Bai, X.F., Zhang, W.J., Fu, L., Xue, T., Bao, L., 2020. Accumulation and exploration of petroleum reservoirs in west slope of northern Songliao Basin, China. Petrol. Explor. Dev. 47 (2), 236–246. https://doi.org/10.1016/S1876-3804(20)60044-1.
- Morley, C.K., 2012. Late cretaceous—early palaeogene tectonic development of SE asia. Earth Sci. Rev. 115 (1), 37–75. https://doi.org/10.1016/j.earscirev.2012.08.002.
- Niu, Y.L., Liu, Y., Xue, Q.Q., Shao, F.L., Chen, S., Duan, M., Guo, P., Gong, H., Hu, Y., Hu, Z., Kong, J., Li, J., Liu, J., Sun, P., Sun, W., Ye, L., Xiao, Y., Zhang, Y., 2015. Exotic origin of the Chinese continental shelf: new insights into the tectonic evolution of the western Pacific and eastern China since the Mesozoic. Sci. Bull. 60 (18), 1598–1616. https://doi.org/10.1007/s11434-015-0891-z.
- Pánek, T., Klimeš, J., 2016. Temporal behavior of deep-seated gravitational slope deformations: a review. Earth Sci. Rev. 156, 14–38. https://doi.org/10.1016/ j.earscirev.2016.02.007.
- Peng, C.S., 2005. Characteristics and evolution of sequence framework in gentle slope zone of dustpan fault basin: a case study of Jiyang depression. J East China Univ Technol. Nat. Sci. 28 (3), 239–243 (in Chinese).
- Peters, K.E., 1986. Guidelines for evaluating petroleum source rock using programmed pyrolysis. K E Peters Search for other works by this author on: GSW Google Scholar 70 (No.3), 318–329. https://doi.org/10.1306/94885688-1704-11d7-8645000102c1865d.
- Qin, Y.X., Shang, Y.N., Fang, Q.X., Fan, Y., 2003. Reservoir collection characteristics of the middlesubmenber of the third member of shahejie Formation in the western slope of gubei depression. Pet Geol Recovery Effic. 10 (b08), 10-11.10.3969/j.issn.1009-9603.2003.z1.005. (in Chinese).
- Quan, Y.B., Chen, Z.Y., Jiang, Y.M., Diao, H., Xie, X., Lu, Y., Du, X., Liu, X., 2022. Hy-drocarbon generation potential, geochemical characteristics, and accumulation contribution of coal-bearing source rocks in the Xihu Sag, East China Sea Shelf Basin. Mar. Petrol. Geol. 136, 105465. https://doi.org/10.1016/j.marpetgeo.2021.105465.
- Shang, L.N., Zhang, X.H., Jia, Y.G., Han, B., Yang, C.S., Geng, W., Pang, Y.M., 2017. Late Cenozoic evolution of the East China continental margin: insights from seismic, gravity, and magnetic analyses. Tectonophysics 698, 1–15. https://doi.org/ 10.1016/j.tecto.2017.01.003.
- Song, Y., Li, Z., Jiang, Z.X., Luo, Q., Liu, D., Gao, Z., 2017. Progress and development trend of unconventional oil and gas geological research. Petrol. Explor. Dev. 44 (4), 675–685. https://doi.org/10.1016/S1876-3804(17)30077-0.
- Su, A., Chen, H., Lei, M., Li, Q., Wang, C., 2019. Paleo-pressure evolution and its origin in the Pinghu slope belt of the Xihu depression, east China Sea Basin. Mar. Petrol. Geol. 107, 198–213. https://doi.org/10.1016/j.marpetgeo.2019.05.017.
- Su, A., Chen, H.H., Lei, C., Chen, X., Wang, P., Wu, T., Chen, J., Chen, H., 2014. Application of PVTxSimulation of fluid inclusions to estimate petroleum charge stages and restore pressure:using Pinghu structural belt in Xihu depression as

- an example. Geol. Sci. Technol. Inf. 33 (6), 137-142 (in Chinese).
- Sun, S.Y., Fan, C.Y., Pu, R.H., Wang, G., Wang, A.G., Huang, L., 2022. Research on vertical sealing of faults in Pinghu structural belt of Xihu Sag. Fault-Block Oil Gas Field 29 (3), 353—359 (in Chinese).
- Suo, Y.H., Li, S.Z., Jin, C., Zhang, Y., Zhou, J., Li, X., Wang, P., Liu, Z., Wang, X., Somerville, I., 2019. Eastward tectonic migration and transition of the Jurassic-Cretaceous Andean-type continental margin along Southeast China. Earth Sci. Rev. 196. https://doi.org/10.1016/j.earscirev.2019.102884.
- Suo, Y.H., Li, S.Z., Zhao, S.J., Somerville, I.D., Yu, S., Dai, L.M., Xu, L.Q., Cao, X.Z., Wang, P.C., 2015. Continental margin basins in East Asia: tectonic implications of the Meso-Cenozoic East China Sea pull-apart basins. Geol. J. 50 (2), 139–156. https://doi.org/10.1002/gj.2535.
- Tong, Y., Ibarra, D.E., Caves, J.K., Mukerji, T., Graham, S.A., 2017. Constraining basin thermal history and petroleum generation using palaeoclimate data in the Piceance Basin, Colorado. Basin Res. 29 (4), 542–553. https://doi.org/10.1111/ hre 12213
- Van den Kerkhof, A.M., Hein, U.F., 2001. Fluid inclusion petrography. Lithos 55 (1), 27–47. https://doi.org/10.1016/S0024-4937(00)00037-2.
- Wang, C., Lv, Y.F., Wang, Q., Fu, G., Wang, Y., Sun, Y., Huo, Z., Liu, J., 2017. Evaluations of oil and gas lateral migration across faults: a case study of Shigezhuang nose structure of Wen'an slope in Baxian sag, Jizhong depression, Bohai Bay Basin, East China. Petrol. Explor. Dev. 44 (6), 932–940. https://doi.org/10.1016/S1876-3804(17)30105-2.
- Wang, F.W., Chen, D.X., Wang, Q.C., Du, W.L., Chang, S., Wang, C., Tian, Z., Cheng, M., Yao, D., 2021. Quantitative evaluation of caprock sealing controlled by fault activity and hydrocarbon accumulation response: K gasfield in the Xihu Depression, East China Sea Basin. Mar. Petrol. Geol. 134, 105352. https://doi.org/10.1016/j.marpetgeo.2021.105352.
- Wang, H.C., Wang, Y.Q., Qin, Y.L., Yang, C.H., Li, L., Lv, Q., Fu, J., 2006. Sedimentary slopes and their hydrocarbon bearing properties in the Bohai Bay Basin. J Geomech 12 (1), 23–30. https://doi.org/10.3969/j.issn.1006-6616.2006.01.004 (in Chinese).
- Wang, K., Chen, L., Xiong, X., Yan, Z., Xie, R., 2020. The role of lithospheric heterogeneities in continental rifting: implications for rift diversity in the North China Craton. J. Geodyn. 139, 101765. https://doi.org/10.1016/ji.jog.2020.101765.
- Wang, W., Bidgoli, T., Yang, X.H., Ye, J.R., 2018. Source-to-Sink links between east asia and taiwan from detrital zircon geochronology of the Oligocene Huagang Formation in the East China Sea Shelf basin. Geochem Geophys Geosyst 19 (10), 3673–3688. https://doi.org/10.1029/2018gc007576.
- Wang, W.G., Lin, C.Y., Zhang, X.G., Dong, C.M., Ren, L., Lin, J., 2020. Effect of burial history on diagenetic and reservoir-forming process of the Oligocene sandstone in Xihu sag, East China Sea Basin. Mar. Petrol. Geol. 112, 104034. https://doi.org/ 10.1016/j.marpetgeo.2019.104034.
- Wang, Y., Qin, Y., Yang, L., Liu, S., Elsworth, D., Zhang, R., 2020. Organic geochemical and petrographic characteristics of the coal measure source rocks of Pinghu Formation in the Xihu sag of the East China Sea Shelf basin: implications for coal measure gas potential. Acta Geol. Sin. 94 (2), 364–375. https://doi.org/ 10.1111/1755-6724.14303.
- Wang, Y.S., Xian, B.Z., 2006. Fault structures of northern steep slope belts and their influences on sedimentation and reservoir formation in Chezhen Sag. Pet Geol Recovery Effic 13 (6), 5–8. https://doi.org/10.3969/j.issn.1009-9603.2006.06.002 (in Chinese).
- Wu, J.P., Wan, L.F., Zhang, L., Wang, Y.M., Zhao, Q., Li, K., Wang, S., 2017. Lithofacies types and sedimentary facies of Pinghu Formation in Xihu depression. Lithol Reservoirs 29 (1), 27–34. https://doi.org/10.3969/j.issn.1673-8926.2017.01.004 (in Chinese).
- Xu, F.H., Xu, G.S., Liu, Y., Zhang, W., Cui, H., Wang, Y., 2020. Factors controlling the development of tight sandstone reservoirs in the Huagang Formation of the central inverted structural belt in Xihu sag, East China Sea Basin. Petrol. Explor. Dev. 47 (1), 101–113. https://doi.org/10.1016/S1876-3804(20)60009-X.
- Xue, Y.A., Yang, H.F., Xu, C.G., 2016. Differential reservoir-controlling effect and hydrocarbon enrichment of slope zone in Huanghekou sag, Bohai Bay Basin. China Pet Explor 21 (4), 65–74. https://doi.org/10.3969/j.issn.1672-7703.2016.04.007 (in Chinese).
- Yan, B., Yuan, H.Q., Shan, X.L., Zhou, T.Q., Liu, S.F., 2022. Sedimentary characteristics and their controlling factors of lower cretaceous fan deltas in saidong sub-sag of saihantala sag, erlian basin, northeastern China. Energies 15 (22). https:// doi.org/10.3390/en15228373.
- Yang, C.Q., Sun, J., Yang, Y.Q., Yang, C.S., Wang, J., Xiao, G., Wang, J., 2020. Key factors controlling mesozoic hydrocarbon accumulation in the southern east China Sea Basin. Mar. Petrol. Geol. 118, 104436. https://doi.org/10.1016/ j.marpetgeo.2020.104436.
- Yang, P.C., Li, H., Liu, F., Li, Q., 2019. Formation mechanism of condensate oil and waxy oil in Structure X of Xihu Depression. Mar. Geol. Quat. Geol. 39 (6), 177–187. https://doi.org/10.16562/j.cnki.0256-1492.2019070405 (in Chinese).
- Yang, Y.C., Xie, X.J., Li, Y.C., Guo, G., Xi, X., Ding, W., 2023. Formation and distribution of coal measure source rocks in the Eocene Pinghu Formation in the Pinghu slope of the Xihu depression, east China Sea Shelf basin. Acta Oceanol. Sin. 42 (3), 254–269. https://doi.org/10.1007/s13131-023-2176-8.
- Yu, X.H., Jiang, H., Li, S.L., Chen, Y.Q., 2007. Depositional flling models and controlling factors on Mesozoic and Cenozoic fault basins of terrestrial facies in eastern China-A case study of Dongying Sag of Jjiyang Depression. Lithol Reservoirs 19 (1), 39–45. https://doi.org/10.3969/j.issn.1673-8926.2007.01.007 (in Chinese).
- Yu, Y.F., Zhang, J.P., Cheng, C., Tang, X.J., Xu, H., 2022. Main controlling factors and

reservoir forming model for hydrocarbon accumulation in the Xihu Sag,the East China Sea Shelf Basin. Marine Geology Frontiers 38 (7), 40–47. https://doi.org/10.16028/j.1009-2722.2021.257 (in Chinese).

- Yu, Z.K., Ding, F., Zhao, H., 2018. Characteristics of structural evolution and classification of hydrocarbon migration and accumulation units in Xihu Sag, China. Shanghai Land and Resources 39 (4), 75–78. https://doi.org/10.3969/j.issn.2095-1329.2018.04.016 (in Chinese).
- Yuan, L.H., 2007. Application of slope break theory in exploration of subtle traps in Wudong slope belt of Hailar Basin. Natural Gas Exploration and Development 30 (3), 29–31. https://doi.org/10.3969/j.issn.1673-3177.2007.03.008 (in Chinese).
- Yuan, X.J., Jiao, H.S., 2002. Exploration of subtle reservoirs in oil and gas sag of Bohai Bay Basin. Oil Gas Geol. 23 (2), 130–133. https://doi.org/10.11743/ogg20020205 (in Chinese).
- Zeng, F., Dong, C.M., Lin, C.Y., Wu, Y., Tian, S., Zhang, X., Lin, J., 2021. Analyzing the effects of multi-scale pore systems on reservoir properties—a case study on Xihu depression, east China Sea Shelf basin, China. J. Petrol. Sci. Eng. 203, 108609. https://doi.org/10.1016/j.petrol.2021.108609.
- Zeng, L.B., Gong, L., Guan, C., Zhang, B.J., Wang, Q.Q., Zeng, Q., Lyu, W.Y., 2022. Natural fractures and their contribution to tight gas conglomerate reservoirs: a case study in the northwestern Sichuan Basin, China. J. Petrol. Sci. Eng. 210, 110028. https://doi.org/10.1016/j.petrol.2021.110028.
- Zhai, G.M., He, W.Y., 2005. Oil and gas exploration direction in China from regional structural background. China Pet Explor 10 (2), 1–8. https://doi.org/10.3969/j.issn.1672-7703.2005.02.001 (in Chinese).
- Zhang, G.H., Li, S.Z., Suo, Y.H., Zhang, J.P., 2016. Cenozoic positive inversion tectonics and its migration in the East China Sea Shelf basin. Geol. J. 51 (S1), 176–187. https://doi.org/10.1002/gj.2809.
- Zhang, J.Y., Lu, Y.C., Krijgsman, W., Liu, J., Li, X., Du, X., Wang, C., Liu, X., Feng, L., Wei, W., Lin, H., 2018. Source to sink transport in the Oligocene Huagang Formation of the Xihu depression, east China Sea Shelf basin. Mar. Petrol. Geol. 98, 733–745. https://doi.org/10.1016/j.marpetgeo.2018.09.014.
- Zhang, J.Y., Zhu, R.K., Wu, S.T., Jiang, X.H., Liu, C., Cai, Y., Zhang, S.R., Zhang, T.S., 2023. Microscopic oil occurrence in high-maturity lacustrine shales: qingshankou formation, gulong sag, songliao basin. Petrol. Sci. https://doi.org/10.1016/ i.petsci.2023.08.026.
- Zhang, P.L., Meng, Q.T., Misch, D., Sachsenhofer, R.F., Liu, Z., Hu, F., Shen, L., 2021. Oil shale potential of the lower cretaceous jiufotang formation, beipiao basin, northeast China. Int. J. Coal Geol. 236, 103640. https://doi.org/10.1016/ j.coal.2020.103640.
- Zhang, P.L., Misch, D., Meng, Q.T., Sachsenhofer, R.F., Liu, Z., Jia, J., Gao, F., Bechtel, A., Hu, F., 2022. Lateral changes of organic matter preservation in the lacustrine Qingshankou Formation (Cretaceous Songliao Basin, NE China): evidence for basin segmentation. Int. J. Coal Geol. 254, 103984. https://doi.org/10.1016/ i.coal.2022.103984.

- Zhang, X.Q., Zhang, G.C., Jiang, Y.M., Cui, M., He, X., 2023. The control of curved faults on structural trap formation: tiantai slope belt, Xihu Sag, East China Sea. Mar. Petrol. Geol. 156, 106464. https://doi.org/10.1016/j.imarpetgeo.2023.106464.
- Zhang, Y., 2005. Structural characteristics and classification of gentle slope belt in Jiyang Depression. Fault-Block Oil Gas Field 12 (3), 22–24. https://doi.org/ 10.3969/j.issn.1005-8907.2005.03.008 (in Chinese).
- Zhang, Y.Z., Hu, S.Q., Liu, J.S., Chen, Z.Y., Jiang, Y., Zou, W., Diao, H., 2022. Gas accumulation conditions and mode in X sag of East China Sea Basin. China Offshore Oil Gas 34 (1), 27–35. https://doi.org/10.11935/j.issn.1673-1506.2022.01.004 (in Chinese).
- Zhao, Q., Zhu, H.T., Zhou, X.H., Liu, Q., Cai, H., Gao, W., 2021. Continental margin sediment dispersal under geomorphic control in Xihu depression, east China Sea Shelf basin. J. Petrol. Sci. Eng. 205, 108738. https://doi.org/10.1016/ i.petrol.2021.108738.
- Zhao, S., Liu, H., Jiang, Y.L., Wang, Y., Hao, X., Zhang, C., 2019. Ramp zone types and their hydrocarbon distribution characteristics in the Bohai Bay Basin. Oil Gas Geol. 40 (2), 223–235. https://doi.org/10.11743/ogg20190202 (in Chinese).
- Zhao, W.Z., Zou, C.N., Wang, Z.C., Li, J., 2004. The intension and signification of "Sagwide Oil-Bearing Theory" in the hydrocarbon-rich depression with terrestrial origin. Petrol. Explor. Dev. 31 (2), 5–13 (in Chinese).
 Zhao, X.Z., Jin, F.M., Li, Y.B., Wang, Q., Zhou, L., Lv, Y., Pu, X., Wang, W., 2016. Slope
- Zhao, X.Z., Jin, F.M., Li, Y.B., Wang, Q., Zhou, L., Lv, Y., Pu, X., Wang, W., 2016. Slope belt types and hydrocarbon migration and accumulation mechanisms in rift basins. Petrol. Explor. Dev. 43 (6), 841–849. https://doi.org/10.1016/S1876-3804(16)30110-0.
- Zhao, X.Z., Zhou, L.H., Pu, X.G., Xiao, D.Q., Jiang, W., Han, W., Chen, C., Zou, L., Guo, S., 2017. Hydrocarbon enrichment theory and exploration practice in the slope of fault lake basin-a case study of Paleogene in Huanghua depression. China Pet Explor 22 (2), 13–24 (in Chinese).
- Zhou, L.H., Han, G.M., Dong, Y.Q., Shi, Q.R., Ma, J., Hu, J., Ren, S., Zhou, K., Wang, J., Si, W., 2019. Fault-Sand combination modes and hydrocarbon accumulation in binhai fault nose of qikou sag, bohai bay basin, east China. Petrol. Explor. Dev. 46 (5), 919–934. https://doi.org/10.1016/S1876-3804(19)60249-1.
- Zhou, X.X., Xiang, L.X., Sui, F.G., Wang, X., Li, Y., 2022. The breakthrough pressure and sealing property of Lower Paleozoic carbonate rocks in the Gucheng area of the Tarim Basin. J. Petrol. Sci. Eng. 208, 109289. https://doi.org/10.1016/ i.petrol.2021.109289.
- Zhu, W.L., Zhong, K., Fu, X.W., Chen, C., Zhang, M., Gao, S., 2019. The formation and evolution of the East China Sea Shelf Basin: a new view. Earth Sci. Rev. 190, 89–111. https://doi.org/10.1016/j.earscirev.2018.12.009.
- Zhu, Y.M., Li, Y., Zhou, J., Gu, S.X., 2012. Geochemical characteristics of Tertiary coalbearing source rocks in Xihu depression, East China Sea basin. Mar. Petrol. Geol. 35 (1), 154–165. https://doi.org/10.1016/j.marpetgeo.2012.01.005.
- Zou, C.N., Tao, S.Z., Xue, S.H., 2005. Connotation of "facies control theory" and its significance for exploration. Petrol. Explor. Dev. 32 (6), 7–12 (in Chinese).